Targeted epigenetic editing of SPDEF reduces mucus production in lung epithelial cells

Song, Juan; Cano-Rodriquez, David; Winkle, Melanie; Gjaltema, Rutger A. F.; Goubert, Desiree; Jurkowski, Tomasz P.; Heijink, Irene H.; Rots, Marianne G.; Hylkema, Machteld N.

Published in:
American Journal of Physiology - Lung Cellular and Molecular Physiology

DOI:
10.1152/ajplung.00059.2016

Publication date:
2017

Targeted epigenetic editing of SPDEF reduces mucus production in lung epithelial cells

Juan Song [1, 2, 3], David Cano Rodriguez [1], Melanie Winkle [1], Rutger A.F. Gjaltema [1], Désirée Goubert [1], Tomasz P. Jurkowski[4], Irene H. Heijink [1, 2], Marianne G. Rots [1, *] and Machteld N. Hylkema [1,2, *]

[1]University of Groningen, University Medical Center Groningen, Department of Pathology and Medical Biology, Groningen, the Netherlands

[2]University of Groningen, University Medical Center Groningen, GRIAC Research Institute, Groningen, the Netherlands

[3]Tianjin Medical University, School of Basic Medical Sciences, Department of Biochemistry and Molecular Biology, Department of Immunology, Tianjin, China

[4]Institute of Biochemistry, Pfaffenwaldring 55, Faculty of Chemistry, University of Stuttgart, D-70569 Stuttgart, Germany

* These authors contributed equally to this work.

Correspondence: Machteld Hylkema, PhD

Department of Pathology and Medical Biology EA10, University Medical Center Groningen, Hanzeplein 1, 9713 GZ Groningen, the Netherlands

Phone: 00 31 50 3619850. Fax: 00 31 50 3619107. E-mail: m.n.hylkema@umcg.nl

Keywords: *SPDEF*, epigenetic editing, mucus production, DNA methylation

Running title: Epigenetic silencing of SPDEF reduces MUC5AC production

Abstract

Airway mucus hypersecretion contributes to the morbidity and mortality in patients with chronic inflammatory lung diseases. Reducing mucus production is crucial for improving patients' quality of life. The transcription factor SAM-pointed domain–containing Ets-like factor (*SPDEF*) plays a critical role in the regulation of mucus production, and therefore represents a potential therapeutic target. This study aims to reduce lung epithelial mucus production by targeted silencing *SPDEF* using the novel strategy epigenetic editing.

Zinc fingers and CRISPR/dCas platforms were engineered to target repressors (KRAB, DNA methyltransferases, histone methyltransferases) to the *SPDEF* promoter.

All constructs were able to effectively suppress both *SPDEF* mRNA and protein expression, which was accompanied by inhibition of downstream mucus-related genes (Anterior gradient 2 (*AGR2*), Mucin 5AC (*MUC5AC)*). For the histone methyltransferase G9A, and not its mutant nor other effectors, the obtained silencing was mitotically stable.

These results indicate efficient *SPDEF* silencing and down regulation of mucus related gene expression by epigenetic editing, in human lung epithelial cells. This opens avenues for epigenetic editing as a novel therapeutic strategy to induce long-lasting mucus inhibition.

Introduction

Airway epithelial mucus secretion and mucociliary clearance plays a key role in protective innate immune responses against inhaled noxious particles and microorganisms. However, excessive mucus production and secretion contributes to the pathogenesis of several chronic inflammatory lung diseases such as asthma and chronic obstructive pulmonary disease (COPD) (9, 11, 27). In patients with asthma and COPD, mucus hypersecretion is associated with cough and sputum production, respiratory infections, accelerated lung function decline, exacerbations and mortality (23, 34). Therefore, targeted treatment of pathologic airway mucus secretion is expected to not only improve symptoms of cough and dyspnea, but also decrease the frequency of disease-related exacerbations and decelerates the disease progression. In the past few years, in preclinical models relevant to COPD, several drugs were shown to reduce mucus hypersecretion (21). However, none of these drugs targeted the mucus producing cell itself.

Airway mucus contains mostly water and secreted mucins that contribute to the viscosity and elasticity of mucus gels. Mucin 5AC (*MUC5AC)* is the major secreted mucin, which is mainly produced by goblet cells in the airway epithelium. In chronic respiratory diseases, mucus hypersecretion is highly associated with increased numbers of goblet cells, as well as up regulated levels of mucin synthesis and secretion (9). SAM pointed domain-containing Ets transcription factor (*SPDEF*) has been reported to be a core transcription factor (TF) that, within a large network of genes, controls mucus production and secretion (6, 22, 35). In lung, *SPDEF* is selectively expressed in goblet cells lining the airways of patients with chronic lung disease (6) and mice exposed to allergens (25). In mice, the absence of *SPDEF* was shown to protect from goblet cell development after allergen exposure (6, 26). Moreover,

knockdown of *SPDEF* with small interfering RNA (siRNA) was found to significantly reduce the expression of IL-13-induced *MUC5AC* expression and Anterior gradient 2 (*AGR2*) expression, which encodes a potential chaperone required for mucin packaging, in the human bronchial epithelial cell line 16HBE (36). These observations suggest that *SPDEF* could be a potential therapeutic target of airway mucus hypersecretion. In this study we set out to silence *SPDEF* expression by epigenetic editing. Epigenetic editing is a novel approach to modulate epigenetic states locally by targeting an epigenetic enzyme to the locus of interest via DNA-targeting systems, such as zinc fingers (ZFs), transcription activator-like effectors (TALEs), or clustered regularly interspaced short palindromic repeats (CRISPRs) (5, 8, 17, 33). Compared to artificial transcription factors (ATFs), which exploit programmable DNA-binding platforms to target transcriptional activators or repressors with no catalytic domain (such as super KRAB Domain, SKD), epigenetic editing has the promise to induce stable and inheritable gene modulation (4, 31). In this study, we provide proof-of-concept that *SPDEF* provides a promising target for epigenetic editing to prevent epithelial *MUC5AC* expression.

Materials and Methods

Cell culture

Human bronchial epithelial 16HBE 14o- (16HBE) and BEAS-2B, mucoepidermoid carcinoma NCI-H292 and type II alveolar carcinoma A549 cell lines were cultured as previously described (15). The human embryonic kidney HEK293T cell line (obtained from American Type Culture Collection (ATCC)) and the breast cancer cell line MCF7 (obtained from ATCC: HTB-22) were cultured in Dulbecco's modified Eagle medium (Biowhittaker, Verviers,

Belgium). All culture media were supplemented with 2 mmol/L L-glutamine, 50 µg/mL gentamicin, and 10% FBS (Biowhittaker).

Plasmids Constructs

Four 18-bp zinc finger (ZF) protein target sites were selected within the *SPDEF* promoter using the website www.zincfingertools.org., as previously described (16). The target sequences are shown in Fig. 2a. The DNA sequences encoding the ZFs were synthesized by Bio Basic Canada. The fragments encoding the ZFs were digested with BamHI/ NheI restriction enzymes (Thermo Fisher Scientific, Carlsbad, USA) and cloned into a SKD-NLS-ZF-TRI FLAG backbone, which encodes SKD, a triple-FLAG tag and a nuclear localization signal (NLS) or a ZF- NLS-VP64-TRI FLAG backbone, which encodes a tetramer of Herpes Simplex Virus Viral Protein 16 (VP64). Then the SKD-NLS-ZF SPDEF-TRI FLAG fragments and the ZF SPDEF- NLS-VP64-TRI FLAG were XbaI/ NotI (Thermo Fisher Scientific) digested and subcloned into a dual promoter lentiviral vector pCDH-EF1-MCS-BGH PCK-GFP-T2A-Puro (SBI, Cat. #CD550A-1), obtaining constructs CD550A-1 SKD-ZF SPDEF and CD550A-1 ZF SPDEF-VP64. To obtain the constructs CD550A-1 ZF SPDEF-DNMT3A, the DNMT3A catalytic domain (kindly provided by Dr. A Jeltsch) was digested out from pMX-ZF-DNMT3A-IRES-GFP with AscI and PacI, to replace VP64 in the CD550A-1 ZF SPDEF-VP64 vector. Catalytically mutant of DNMT3A (E74A) (13) was generated by PCR-mediated site directed mutagenesis on CD550A-1 ZF SPDEF-DNMT3A. To obtain the constructs CD550A-1 ZF SPDEF-G9a and CD550A-1 ZF SPDEF-G9a W1050A, the G9a catalytic domain and its mutant was digested out from pMX-E2C-G9a and pMX-E2C-G9a W1050A (10) with AscI and PacI, to replace VP64 in the CD550A-1 ZF SPDEF-VP64. To construct the CD550A-1 ZF SPDEF without effector

domains (EDs) (SPDEF-NOED), VP64 in the CD550A-1 ZF SPDEF-VP64 was swapped out with PCR by a multiple cloning site, including restriction sites for AscI, NsiI, BclI, SwaI, and PacI. The primer information is presented in Table 1. pHAGE EF1α dCas9-VP64 lentiviral construct was a gift from Rene Maehr & Scot Wolfe (Addgene plasmid # 50918)(18) and the single-chain guide RNA encoding plasmid MLM3636 was a gift from Keith Joung (Addgene plasmid # 43860). An additional multiple cloning site was added by replacing the VP64 activator with a sequence containing a MluI restriction site. To obtain the dCas9-epigenetic editor constructs, the G9a catalytic domain and its mutant, the SUV39h1 catalytic domain (10), and the catalytic domain of EZH2 (SET) and its mutant were digested out from pMX-ZF-IRES-GFP with MluI and NotI and subcloned into the empty pHAGE EF1α dCas9. The SKD domain and the DNMT3A3L catalytic domain and its catalytic mutant (29) were subcloned by amplifying with primers containing MluI and NotI overhangs. Cloning of guide RNAs (gRNA) was achieved as previously described (4). Briefly, pairs of DNA oligonucleotides encoding 20 nucleotide gRNA targeting sequences were annealed together to create double-stranded DNA fragments with 4-bp overhangs. These fragments were ligated into BsmBI-digested plasmid pMLM3636. Two gRNAs were designed to bind close to the region where ZF3 and ZF4 bind (Fig. 2A) (GCATGGATCCCCCAGCAAGG and CCTCAGGTTGGGCCTTGCCA, respectively) and a third gRNA was designed to bind just before transcription start site (CTGGCCAACTCTTCATCTCG). We verified all constructs by DNA Sanger sequencing (Baseclear, Leiden, the Netherlands).

Lentiviral transduction

The lentiviral CD550A-1 constructs, encoding the *SPDEF* targeting ATFs and epigenetic editors, were co-transfected with the third generation packaging plasmids pMDLg/pRRE, pRSV-Rev, pMSV-VSVG into HEK293T cells using the calcium phosphate transfection method to produce lentiviral particles. The supernatant of HEK293T cells containing virus was harvested at 48 and 72 hours after transfection. Host A549 cells were seeded in six-well plates with a density of 80,000 cells per well and transduced on two consecutive days with the viral supernatant, supplemented with 8 μg/mL polybrene (Sigma-Alrich, Zwijndrecht, Netherlands). The positive transduced cells were selected in 8 μg/mL puromycin supplemented medium for four days from 72h after the last transduction and then were cultured in 1 μg/mL puromycin supplemented medium. Medium was refreshed every 2-3 days. Ten days after the last transduction, cells were harvested for western blot, as well as RNA and DNA extraction. In the meantime, cells were grown on coverslips for immunocytochemistry (IHC) and harvested for chromatin immunoprecipitation.

Generation of MCF7 stable cell lines

The lentiviral pHAGE-EF1α constructs, encoding the dCas9-SKD and epigenetic editors, were co-transfected with the second generation packaging plasmids psPAX2 and pMD2.G-VSV-G into HEK293T cells using Lipofectamine LTX-PLUS (Life Technologies) to produce lentiviral particles. The supernatant of HEK293T cells containing virus was harvested at 48 and 72 hours after transfection. Host MCF7 cells were seeded in six-well plates with a density of

80,000 cells per well and transduced on two consecutive days with the viral supernatant, supplemented with 8 µg/mL polybrene (Sigma-Alrich, Zwijndrecht, Netherlands). The positive transduced cells were selected in 8 µg/mL puromycin supplemented medium for four days from 72h after the last transduction and then were cultured in 1 µg/mL puromycin supplemented medium.

gRNA Transfections

To transiently transfect the MLM3636 plasmids containing gRNA constructs, 500,000 of each stable MCF7 cells were seeded into 6-well plates the day before transfection. For all experiments, a total of 2 µg of a combination of three gRNA plasmids were cotransfected using 2 µl PLUS reagent and 4 µl Lipofectamine LTX. The cells were then collected two days after transfection to isolate RNA and subcultured for additional 12 days.

Detection of mRNA expression by quantitative real-time PCR

Total RNA was extracted from A549 cells using Trizol reagent (Thermo Fisher Scientific) and 500 ng was used for cDNA synthesis with random primers using Superscript II RNase H - Reverse transcriptase (Thermo Fisher Scientific). *SPDEF*, *MUC5AC*, *AGR2* and *GAPDH* expression was quantified using qPCR MasterMix Plus (Eurogentec, Belgium) and Taqman gene expression assays (*SPDEF*: Hs01026050_m1; *MUC5AC*: Hs00873651_Mh; *AGR2*: Hs00356521_m1; *GAPDH*: Hs02758991_g1, Thermo Fisher Scientific), mRNA expression of the fusion proteins (FLAG tag), Procollagen-Lysine,2-Oxoglutarate 5-Dioxygenase 2 (*PLOD2*), Tumor Protein P53 (*TP53*), RELA Proto-Oncogene, NF-KB Subunit (*RELA*), Cyclin Dependent Kinase Inhibitor 1A (*CDKN1A*) and beta-actin (*ACTB*) using SYBR® Green PCR Master Mix

(Thermo Fisher Scientific) and gene-specific primers (Table 1) with the LightCycler® 480 Real-Time PCR System (Roche, Basel, Switzerland). Data were analyzed with LightCycler® 480 SW 1.5 software (Roche) and the Fit points method, according to the manufacturer's instructions. Expression levels relative to *GAPDH* were determined with the formula $2^{-\Delta Cp}$ (Cp means crossing points).

Methylation analysis by pyrosequencing

For DNA methylation analysis of the target regions, genomic DNA was extracted with chloroform-isopropanol and was bisulfite converted using the EZ DNA Methylation-Kit (Zymo Research), following the manufacturer's protocol. Bisulfite-converted DNA was analyzed by pyrosequencing as previously described (7). The primer information for pyrosequencing is presented in Table 1.

Histone modification analysis by chromatin immunoprecipitation and qPCR

Histone modification induced by ZFs-G9a was analyzed by ChIP as previously described (12). Briefly, A549 cells were fixed with 1% formaldehyde at 37 °C for 10 min and subsequently lysed and sonicated using a Bioruptor (Diagenode; High, 30 sec on, 30 sec off, total time 15 minutes). Sheared chromatin was cleared by centrifuge at 4°C (12,000 × g, 10 minutes). Four microgram of specific antibodies [normal rabbit IgG (abcam, ab46540), H3K9me2 (Milipore, 07-441)] were bound to 50 µl of magnetic Dynabeads (Thermo Fisher Scientific) during 15 minutes incubation, then unbound antibodies were washed-off. Sheared chromatin 0.25 million cells was added to the antibody precoated magnetic Dynabeads (rotating overnight

196 at 4°C). Next day, the magnetic Dynabeads were washed three times with PBS, and
197 chromatin was eluted with 1% (w/v) SDS and 100 mmol/L NaHCO3. Subsequently, the
198 elutes were treated with RNase (Roche) for four hours and proteinase K (Roche) for one
199 hour at 62°C. Then, the column (Qiagen) purified DNA could be analyzed with quantitative
200 PCR (qPCR).
201 To assess the induction of histone marks and their spreading, several primer pairs were used
202 for the SPDEF promoter (Table 1). qPCR was conducted using SYBR Green PCR Master Mix
203 (Thermo Fisher Scientific) on an LightCycler® 480 Real-Time PCR System (Roche). To
204 calculate the fold induction/reduction of histone marks we used the formula: Percentage
205 input = $2^{(Cpinput-CpChIP)}$ dilution × factor × 100.
206

207 **Detection of protein expression by western blot**

208 Transduced A549 cells were lysed in RIPA buffer and proteins were analyzed by standard
209 western blotting as previously described (7). Then, the blots were incubated with a rabbit
210 anti-human SPDEF antibody (Santa Cruz, sc-67022), mouse anti-FLAG (Sigma, F3165) and
211 mouse anti-GAPDH (Santa Cruz, sc-47724) at 4°C, overnight, followed by incubation with an
212 horseradish peroxidase (HRP)-conjugated secondary goat anti-rabbit and rabbit anti-mouse
213 antibody (Dako, Glostrup, Denmark). Protein expression was visualized using the Pierce ECL2
214 chemoluminescence detection kit (Thermo Fisher Scientific) and Gel Doc™ XR+ imaging
215 systems (Bio-Rad Laboratories). Data were analyzed with Gel Doc™ XR+ Image Lab™
216 software.

Immunocytochemistry

Cells grown on coverslips (Menzel-Gläser, 12 mm in diameter) were washed with PBS and fixed with 2% (w/v) Paraformaldehyde for 20 min. Cells were stained with primary antibody against MUC5AC (Abcam, ab3649), followed by HRP-conjugated secondary antibody. The peroxidase was visualized by staining with AEC (3-amino-9 ethylcarbazole), followed by hematoxylin counterstaining. The cover glasses were mounted with Kaiser's glycerol-gelatin (37°C) and scanned into digital whole slides images using the NanoZoomer series scanning devices. The assessment of immunochemistry staining intensity was performed semiquantitatively in a blinded fashion at four to six of x20 magnification fields. MUC5AC stained cells were categorized as follows: negative (no staining), weak-positive (pink color or small red dot staining) and strong-positive (red staining and >50% of cell volume).
FLAG tagged proteins were stained with anti-FLAG antibody (Sigma, F3165), followed by HRP-conjugated secondary antibody and AEC staining. FLAG stained cells were categorized to negative and positive, and counted in a blinded fashion at four x20 magnification fields.

Statistics

All transduction experiments were performed at least three times independently. Data were analyzed using one-way ANOVA followed by Bonferroni's Multiple Comparison Test. Data were considered to be statistically significant if $P<0.05$. Data were expressed as mean ± SEM and calculated using Prism v5.0 (GraphPad software).

Results

SPDEF down regulation by ATFs and subsequent repression of mucus-related genes

To select a suitable model to study *SPDEF* down regulation, *SPDEF* expression was determined in four different human epithelial cell lines: A549, H292, BEAS-2B and 16HBE. A549 cells demonstrated the highest expression of *SPDEF*, both at mRNA level (Fig. 1A) and at protein level (Fig. 1B). The high expression of *SPDEF* in A549 and H292 cells was accompanied by a low degree of DNA methylation at the CpG sites surrounding the transcription start site (TSS) (A549: CpG sites #13: 2.7%, CpG sites #14: 4.6%, CpG sites #15: 3.1%; H292: CpG sites #13: 1.9%, CpG sites #14: 4.2%, CpG sites #15: 3.2%), whereas the undetectable transcription levels of *SPDEF* in BEAS-2B and 16HBE were accompanied by a high level of DNA methylation (BEAS-2B: CpG sites #13: 34.9%, CpG sites #14: 40.6%, CpG sites #15: 26.4%; 16HBE: CpG sites #13: 75.9%, CpG sites #14: 68.5%, CpG sites #15: 41.0%) (Fig. 1D). Differential expression of *MUC5AC* was consistent with the observed *SPDEF* expression, with the highest *MUC5AC* expression in A549 cells (Fig. 1C). To explore effective *SPDEF* down regulation, we chose the highest *SPDEF* and *MUC5AC* expressing cell line (A549) as a model.

In order to down regulate *SPDEF* expression, four ZFs were designed to bind 18-base pair regions in the *SPDEF* promoter (SPDEF1, SPDEF2, SPDEF3, SPDEF4) and were sub-cloned into lentiviral constructs containing SKD (Fig. 2A). A549 cells were transduced to express the ATF using these lentiviral constructs. To enrich for cells expressing the ATF, the lentiviral transduced cells were positively selected based on puromycin resistance. Correct size of ATFs was confirmed by western blot (Fig. 2C) and their nuclear location by immunohistochemical staining (Fig. 3D). FLAG positive cells ranged from 15% (SKD-SPDEF2)

to 64% (SKD-SPDEF3) after the selection with puromycin (Fig 3D). According to the FLAG staining, SKD-SPDEF1 was expressed to a similar degree as SKD-SPDEF2, and both were generally lower expressed than SKD-SPDEF3 and SKD-SPDEF4.

Next, we examined the ability of the four ATFs to down regulate *SPDEF* mRNA expression in A549 cells. As shown in Fig. 2B, all four ATFs significantly down regulated *SPDEF* expression, demonstrating 70, 97, 93, and 96% respectively down regulation relative to empty vector control, which was confirmed at the protein level (Fig. 2C).

As *SPDEF* regulates a network of genes associated with mucus production (2, 20, 28), we investigated whether the down regulation of *SPDEF* expression mediated by ATFs indeed resulted in reduced expression of mucus-related genes. Therefore, the expression level of two downstream mucus-related genes was investigated in the ATF-expressing A549 cells. We found that expression of *AGR2* was significantly down regulated by SKD-SPDEF2 (90.9%±35.4% repression), SKD-SPDEF3 (79.3%±35.9% repression) and SKD-SPDEF4 (86.2%±35.4% repression) (Fig. 3A). *MUC5AC* was consistently, yet not significantly, down regulated in response to *SPDEF* repression (Fig. 3B). However, MUC5AC immunochemistry staining on ATF-transduced A549 cells supports successful inhibition at the protein level (Fig. 3C and 3D).

SPDEF **silencing by targeted epigenetic editing**

In order to achieve the stable gene silencing, we set out to direct DNA methylation onto the *SPDEF* promoter. As DNA methylation levels of CpG sites #13 (-3 bp), #14 (-1 bp) and #15 (+40 bp) around the TSS negatively correlated with *SPDEF* expression, ZF SPDEF3 targeting location -131 to -114 bp was coupled to the catalytic domain of DNMT3A. To investigate the

induced DNA methylation in the promoter region of *SPDEF*, 15 CpG sites were screened with pyrosequencing (Fig. 4). We found that DNA methylation was induced on CpGs sites #14 and 15, and not on CpG sites #1-13. In further experiments, CpG sites #13-15 were analyzed. SPDEF3-DNMT3A consistently deposited DNA methylation onto two CpG sites (CpG #14: 6.6 ± 0.8%; CpG #15: 10.5 ± 1.3%), compared with SPDEF3-NOED (CpG #site 14: 3.9 ± 0.3%; CpG #15: 5.2 ± 0.8%) (Fig. 5B). To determine whether the observed increase in DNA methylation was directly caused by the catalytic activity of the DNMT3A enzyme, a catalytic mutant of DNMT3A (DNMT3A E74A) was constructed and compared to DNMT3A in a separate set of experiments. No increase in DNA methylation was observed for CpG sites #13-15 in SPDEF3-DNMT3A E74A treated cells (Fig. 5C). To investigate whether the ZF directed DNMT3A was able to reduce target gene transcription, *SPDEF* mRNA expression was investigated (Fig. 6A, left panel). SPDEF3-DNMT3A was able to down regulate *SPDEF* expression (76.6%±25.5% repression), which was equally efficient as repression induced by the positive control SKD-SPDEF3 (79.1%±12.7% repression). Interestingly, the construct that lacked the effector domain, SPDEF3-NOED, also reduced *SPDEF* expression significantly (72.0%±25.3% repression). To determine the influence of location, another ZF (SPDEF4: target sequence +112 to +129) was tested to target DNMT3A to the *SPDEF* promoter. We found that SPDEF4-DNMT3A was able to better down regulate *SPDEF* expression (86.9%±12.1% repression) than control SPDEF4-NOED (46.8%±35.1% *SPDEF* repression) and the catalytic mutant (Fig. 6A), even though SPDEF4-DNMT3A didn't induce methylation changes in the investigated region CpG13-15 (Fig. 5D).

Upon ZFs fused with the histone methyltransferase G9A, again, SPDEF4-G9A was able to down regulate *SPDEF* expression equally efficiently as positive control SKD-SPDEF4 and further repressed *SPDEF* expression than SPDEF4-NOED (Fig. 6A) However, no difference

was detected between SPDEF4-G9A and its mutant and no H3K9me2 marks were detected in the examined region (data not shown). The expression of the fusion proteins was confirmed by the mRNA expression of the FLAG-tag (Fig. 7). The SPDEF4-DNMT3A construct was not higher expressed than its mutant, indicating that enhanced *SPDEF* repression of SPDEF4-DNMT3A compared to its mutant was not because of more occupation of ZFs SPDEF4 itself.

Down regulation of *SPDEF* by SPDEF3-DNMT3A, SPDEF4-DNMT3A, SPDEF3-G9A and SPDEF4-G9A was confirmed at the protein level by western blot (Fig. 8). Importantly, expression of downstream mucus related genes *AGR2* and *MUC5AC* was also down regulated by these constructs (Fig. 6B and 6C).

Lower number of strong MUC5AC positive cells after targeted silencing *SPDEF* by epigenetic editing

The effect of *SPDEF* inhibition on mucus production was determined by quantification of the number of MUC5AC positive cells. Transduced A549 cells were seeded on cover slips and examined by immunochemistry staining. Interestingly, *SPDEF* silencing was most effective within the MUC5AC strong positive cell population. Within this population, both SPDEF3-DNMT3A and SPDEF4-G9a treatment resulted in lower numbers of MUC5AC strong positive (Fig. 9B). To rule out that the effects were caused by a general repressive effect of either G9A or DNMT3A, we determined expression levels of four irrelevant genes (*PLOD2*, *TP53*, *RELA* and *CDKN1A*) and found that none of these demonstrated inhibition of expression (Fig. 10).

Sustained epigenetic repression of *SPDEF* by epigenetic editing

To further address the effectiveness and sustainability of gene repression by epigenetic editing, we decided to use the CRISPR-dCas9 system. We engineered stable MCF7 cell lines, each one expressing dCas9 fusions either with the transcriptional repressor SKD, several epigenetic editors or their mutants (G9a and SUV39h1 (for H3K9me), the SET domain of EZH2 (for H3K27me), or a chimeric DNMT3a-DNMT3L fusion (for DNA methylation(30))). We designed three gRNAs to bind around the promoter of SPDEF. By transiently transfecting a mix of the three gRNAs into the stable cell lines, we were able to address the maintenance of gene repression (Fig. 11A). Gene repression was achieved to similar degrees two days after transfecting the mix of gRNAs in all stable cell lines. As observed for ZF-fusions, repression was also observed when using the mutant effector domains (Figs. 11 B-E). Importantly, for several other genes no such repressive effects by dCas9 without effector domain have been observed in this stable system (data not shown). While repression by the transcriptional repressor SKD and most of the epigenetic editors was not maintained, the repression of SPDEF was sustained when using the G9a effector domain, while the mutant fusion regained activation.

Discussion

Based on its important role in goblet cell differentiation and mucus production (6, 26), we reasoned that *SPDEF* could be a suitable therapeutic target against mucus hypersecretion. In this study, we were able to silence *SPDEF* expression in the human alveolar epithelial cell line A549, using a novel strategy: engineered *SPDEF* targeting ZF proteins directing transcriptional repressor (SKD), as well as epigenetic enzymes (DNMT3A and G9A). The

repression of *SPDEF* was accompanied by lower expression of mucus-related genes *MUC5AC* and *AGR2*, as well as lower numbers of MUC5AC positive cells.

Our data provides an original proof-of-concept study supporting *SPDEF* as a promising therapeutic target for inhibiting mucus production, which is amenable to stable repression with epigenetic editing. As previously reported, knockdown of *SPDEF* using siRNA was able to reduce the IL-13-induced expression of MUC5AC and AGR2 in human airway epithelial 16HBE cells (36). The principle of siRNA is to target and degrade mRNA. Because of the constant production of mRNA, the silencing effect of siRNA is generally transient and it has to be delivered repeatedly in clinical application. Epigenetic editing would be a superior strategy because the effect would be sustained after clearance of the drug (hit and run approach) (8). In order to down-regulate SPDEF expression directly at the transcriptional level, four sequence-specific ZFs were generated. ZFs were first linked to SKD to test the functionality of the DNA binding domain because SKD can cause transient gene silencing by indirectly recruiting chromatin remodelers and histone-modifying enzymes (28, 32). These four ATFs (ZF-SKD) strongly reduced *SPDEF* expression and nearly abolished all expression of *SPDEF* in A549 cells. More importantly, *SPDEF* silencing resulted in the additional down regulation of MUC5AC mRNA and protein expression as well, indicating successful inhibition of mucin synthesis.

Next, ZFs were fused to catalytic domains of epigenetic enzymes (DNMT3A and G9A), aiming for longer term gene silencing by changing the epigenetic state of the targeted gene. ZF-targeted DNA methylation was recently successfully used for silencing several cancer-associated genes, including VEGF-A, SOXA2, and EpCAM (24, 28, 29, 31). Here, we took advantage of this approach by using two different ZFs engineered close to the TSS (SPDEF3

and SPDEF4), to down regulate *SPDEF* expression. In this area, high expression of *SPDEF* was accompanied by lower DNA methylation of CpG sites, particularly those surrounding the TSS, where DNA methylation is tightly linked to transcriptional silencing (3). The occlusion binding of TF also explains our observation that ZFs without effector domains effectively silenced *SPDEF* expression. We observed similar strong SPDEF repressive effects upon targeting ZFs without any effector domain as upon targeting ZFs fused with repressor SKDs. Many factors can explain the repressive effects of the binding of the gene targeting constructs, like competition with endogenous transcription factors, such as SMAD, or components of the preinitiation complex formation. Importantly, the effects were also obtained when targeting CRISPR-dCas9 without an effector by the sgRNAs (20), indicating that steric hindrance might indeed explain the repressive effect. Since such effects generally are transient, it is important to assess that addition of domains to the targeting moiety do not affect inhibition properties. Importantly, the fusion of effector domains to the ZFs did not hamper the repressive effect of the ZF approach.

As the DNA binding domain by itself, or in fusion with SKD, is not expected to induce any long-term effects, we next set out to test different epigenetic enzymes (DNMT3A and G9A). Fusion of epigenetic effector domains with ZFs resulted in the same magnitude of silencing as the ZF-SKD fusions, indicating that our approach worked as we aimed for. Furthermore, targeted DNA methylation or histone methylation has the advantage that its effect has the potential to be permanent (4, 28, 31), albeit the stability and heritability of epigenetic editing is still controversial (14, 19) and likely depend on the local chromatin modification state (4).

In an elegant experiment, Bintu and colleagues used an artificial system to compare four repressive chromatin regulators with distinct chromatin modifications (2): the embryonic ectoderm development (EED) protein of Polycomb repressive complex 2, which indirectly catalyzes H3K27 methylation, the KRAB domain, that indirectly promotes H3K9 methylation, the DNMT3B, that catalyzes DNA methylation and the histone deacetylase 4 (HDAC4) enzyme. By transiently recruiting each protein, they demonstrate that different types of repressed chromatin are generally associated with distinct time scales of repression. For this artificial context, DNA methylation was the modification of choice to achieve long lasting repression, while histone deacetylation was not sustained. Only few studies so far have addressed stable silencing of endogenous genes, and controversial effects have been reported (1, 19, 31). Here, we provide indications that targeting epigenetic effector domains to *SPDEF* has the ability to promote sustained gene expression reprogramming. Indeed, we demonstrated that upon targeting G9A, maintenance of repression was obtained, which was not observed for the transcriptional repressor SKD, DNA methyltransferase or other histone modifiers. These differences in maintenance require more thorough investigations, but likely are due to the particular local chromatin context of the targeted locus, that could influence the potency and longevity of epigenetic reprogramming. This would also explain the reported failure of maintenance of induced H3K9methylation effects when studying VEGF-A repression (19). Combining different effector domains, as we did previously for re-activation of gene expression, might further improve the degree of repression and/or increase sustainability (4). Indeed, Amabile et al recently demonstrated the importance of co-targeting KRAB, DNMT3A and DNMT3L in inducing maintained repression for endogenous genes (1).

One limitation of our study is that functional experiments were conducted in the alveolar cell line A549. Since we already showed convincing *MUC5AC* and *AGR2* silencing in A549 cells, it will be interesting to investigate whether this effect is also observed within the more relevant models of mucus hypersecretion in the future, such as using the air-liquid interface culture of the primary airway epithelial cells from patients with COPD. In addition, before use in the clinical setting, it is necessary to further evaluate the off-target effects, such as the ZFs or CRISPR/dCas9 binding specificity and target cell specificity.

In summary, we successfully reduced mucus-related gene expression by targeted silencing of *SPDEF.* This new approach (epigenetic editing) has the potential to induce a permanent anti-mucus effect, which has implications for development of novel therapeutic strategies to treat patients with chronic mucus hypersecretion in the future.

Acknowledgements

The authors would like to thank, JM Dokter-Fokkens, PG Jellema, MGP van der Wijst, and K Meyer, Department of Pathology and Medical Biology, University Medical Center Groningen (UMCG), for technical help with this study.

Support statement: This work was supported by grants from the Stichting Astma Bestrijding (project 2014/007) and the Jan Kornelis de Cock Stichting (project 2014-62). JS is supported by the Abel Tasman Talent Program, University Medical Center Groningen. DCR is supported by Samenwerkingsverband Noord-Nederland SNN-4D22C-T2007. DG is supported by EU funding H2020-MSCA-ITN-2014-ETN 642691 EpiPredict. TPJ is supported by Baden-Württemberg Stiftung (95011370). MH is MC member of COST (Cooperation in Science and Technology) Action BM1201. MGR is vice-chair of COST Action CM 1406 (EpiChemBio.eu).

Conflict of interest: None declared.

448 Table 1 PCR and sequencing primers

Primer Name	Sequence (5'- 3')	Application
SPDEF Pyro-A F	GGGTTATGGGAGAGTAAGTTGT	PCR and sequencing for SPDEF-A pyrosequencing
SPDEF Pyro-A R	[Biotin]TCTATACCCCACAAAATCCTCAT	
SPDEF Pyro-A Seq	GTTGTTGGTTGGTTT	
SPDEF Pyro-B/C F	GGATTTTGTGGGGTATAGAGAA	PCR and sequencing for SPDEF-B/C pyrosequencing
SPDEF Pyro-B/C R	[Biotin]ATTACTACATAACCACTCAACTCATATT	
SPDEF Pyro-B Seq	GGGGTATAGAGAATATAGTT	
SPDEF Pyro-C Seq	TTTAGAATTTTAGTTTTGGATTTA	
SPDEF Pyro-D/E F	ATGAGTTGAGTGGTTATGTAGTAAT	PCR and sequencing for SPDEF-D/E pyrosequencing
SPDEF Pyro-D/E R	[Biotin]CCAACCCAAAACTACCTACTAAC	
SPDEF Pyro-D Seq	AGTGGTTATGTAGTAATTAATG	
SPDEF Pyro-E Seq	AATTAGGTTTTGGTTAATTT	
DNMT3a-E74A F	CATTGCCTCCGCCGTGTGTGAGG	PCR for DNMT3a-E74A site mutagenesis
DNMT3a-E74A R	TAGCGGTCCACTTGGATGC	
NOED F	CGCGCCATGCATGATCATTTAAATTTAAT	PCR for NOED cloning
NOED R	TAAATTTAAATGATCATGCATGG	
SPDEF-ChIP-region 1 F	GCATGGGTGGTTCTGGATCT	ChIP-qRT-PCR for SPDEF region 1
SPDEF-ChIP-region 1 R	GCCAGAGATACGTCGAGTGG	
SPDEF-ChIP-region 2 F	GCAGCAACCAATGAACGAGTG	ChIP-qRT-PCR for SPDEF region 2
SPDEF-ChIP-region 2 R	ATTAACCCTTGCAGGTCTCCC	

SPDEF-ChIP-region 3 F	CCAGCACATTCCTGCACTCT	ChIP-qRT-PCR for SPDEF region 3
SPDEF-ChIP-region 3 R	CAACCTGAGGGGCTTGCAG	
FLAG-F	TGAATCGGTAGGAATTCGCGG	qRT-PCR for *FLAG*
FLAG-R	GGGAGGGGCAAACAACAGAT	
GAPDH-F	CCACATCGCTCAGACACCAT	qRT-PCR for *GAPDH*
GAPDH-R	GCGCCCAATACGACCAAAT	
ACTB-F	CCAACCGCGAGAAGATGA	qRT-PCR for *ACTB*
ACTB-R	CCAGAGGCGTACAGGGATAG	
RELA-F	CGGGATGGCTTCTATGAGG	qRT-PCR for *RELA*
RELA-R	CTCCAGGTCCCGCTTCTT	
TP53-F	GCTCAAGACTGGCGCTAAAA	qRT-PCR for *TP53*
TP53-R	GTCACCGTCGTGGAAAGC	
PLOD2-F	GGGAGTTCATTGCACCAGTT	qRT-PCR for *PLOD2*
PLOD2-R	GAGGACGAAGAGAACGC	
CDKN1A-F	TCACTGTCTTGTACCCTTGTGC	qRT-PCR for *CDKN1A*
CDKN1A-R	GGCGTTTGGAGTGGTAGAAA	

449

450

Figure legends

Figure 1 Expression of *SPDEF* (mRNA and protein) is associated with DNA methylation and *MUC5AC* expression. Quantification of the mRNA levels of *SPDEF (A)* and *MUC5AC* (C) in a panel of human epithelial cell lines (A549, H292, BEAS-2B, and 16HBE) by qRT-PCR. Dot plots represent the mean and variation of three independent experiments. (B) Visualization of SPDEF protein expression (left) and quantification relative to β-ACTIN (right), as conducted by western blot (n=1). An anti-β-ACTIN antibody was used as a loading control. (D) Quantitative analysis of the methylation levels of three CpG sites surrounding transcription start site (TSS) by pyrosequencing. Scatter plots show two independent experiments.

Figure 2 *SPDEF*-targeted silencing by ATFs in A549 cells. (A) Schematic representations of the promoter region of the *SPDEF* gene, outlining the putative binding sites for transcription factors (STAT6, NKX2-1/NKX3-1, GFI, FOXA1/FOXA2, SMAD) (MatInspector) and the target sequences of zinc fingers: SPDEF1, SPDEF2, SPDEF3, and SPDEF4. Arrows show the orientation of the 18-bp binding site in the promoter. Location of ZF was shown relative to the TSS (+1). The translation start site was shown as ATG (+286). CpGs are indicated as vertical bars. DNA methylation status of 15 CpGs was analyzed using pyrosequencing for the indicated areas. Histone modification of H3K9me2 was assessed for the ChIP regions (gray boxs). (B) Relative *SPDEF* mRNA expression, normalized to the empty vector, assessed by quantitative RT-PCR in transduced A549 cells. Data are presented as mean and variation of three independent experiments. Statistical significance was analyzed using one-way ANOVA followed by Bonferroni's Multiple Comparison Test (*P<0.05, **P<0.01). (C) SPDEF protein expression in transduced A549 cells, as conducted by western blot. An anti- Glyceraldehyde 3-phosphate dehydrogenase (GAPDH) antibody was used as a loading control. An anti-FLAG

antibody was used to detect the ATFs, which were designed with a C-terminal 3×FLAG tag. Blot pictures shown are representative of two independent experiments.

Figure 3 Changes in downstream mucus-related genes after ATFs induced silencing of *SPDEF*. (A) *MUC5AC* and (B) *AGR2* mRNA expression were investigated by quantitative RT-PCR. Data are presented as mean and variation of three independent experiments. Statistical significance was analyzed using one-way ANOVA followed by Bonferroni's Multiple Comparison Test (*P<0.05, **P<0.01). (C)Quantification of MUC5AC negative, weak- and strong-positive A549 cells after ATF treatment. Counting of cells was performed in a blinded fashion. Solid bars, strong positive; shaded bars, weak positive; open bars, negative. Results represent the average of two independent experiments. (D) Representative photographs (original magnification, ×20) from immunochemistry staining for MUC5AC (upper panel) and FLAG (lower panel) in ATFs treated A549 cells. Red-stained cells are MUC5AC-positive and FLAG-positive respectively. Nuclei were counterstained with hematoxylin. Scale bar: 100 μm.

Figure 4 Screening of the DNA methylation changes after targeting DNMT3A to *SPDEF* promoter. Quantitative analysis is the percentage of methylation for 14 CpG sites in *SPDEF* promoter by pyrosequencing in A549 cells treated with mock, empty vector, SPDEF3-NOED and SPDEF3-DNMT3A in one experiment. (A) CpG sites #1, #3, and #4; (B) CpG sites #5-8; (C) CpG sites #9-12; (D) CpG sites #13-15.

Figure 5 DNA methylation changes after targeting DNMT3A to *SPDEF* promoter. (A) Schematic presentation of SPDEF3-DNMT3A and SPDEF4-DNMT3A, and their binding location relative to TSS. (B) Quantitative analysis the percentage of methylation for target CpG sites (#13, #14 and #15) by pyrosequencing in A549 cells treated with mock, empty vector, SPDEF3-NOED and SPDEF3-DNMT3A (n=4). (C) Relative DNA methylation level of

A549 cells after treatment with SPDEF3-NOED, SPDEF3-DNMT3A and SPDEF3-DNMT3A E74A normalized to SPDEF3-NOED (n=3). (D) Relative DNA methylation level of A549 cells after treatment with SPDEF4-NOED, SPDEF4-DNMT3A and SPDEF4-DNMT3A E74A normalized to SPDEF4-NOED (n=3). Dot plots represent the mean and variation of at least three independent experiments. Statistical significance was analyzed using one-way ANOVA followed by Bonferroni's Multiple Comparison Test (*P<0.05, compared to empty vector; #P<0.05, ##P<0.01, compared between two indicated columns).

Figure 6 *SPDEF* and downstream mucus related genes expression changes after targeting DNMT3A and G9a to *SPDEF* promoter. A549 cells were treated with ZFs fused with different effector domains (SKD, DNMT3A, G9a, and the respective mutants DNMT3A E74A and G9a W1050A). mRNA level of (A) *SPDEF*, (B) *AGR2* and (C) *MUC5AC* were determined by quantitative RT-PCR on treated A549 cells. The expression of *SPDEF* was relative to *GAPDH* and normalized to mock treated cells (left panel), or normalized to ZF-NOED (middle and right panels) to enlarge any difference between wild type and mutant effectors. Dot plots represent the mean and variation of at least three independent experiments. Statistical significance was analyzed using one-way ANOVA followed by Bonferroni's Multiple Comparison Test (*P<0.05, **P<0.01, ***P<0.001, compared to empty vector; #P<0.05, ##P<0.01, ###P<0.001, compared between two indicated columns).

Figure 7 Expression of ZF-ED after A549 cells treated with ZF fused to different effector domain (SKD, DNMT3A, G9a, and respective mutant DNMT3A E74A and G9a W1050A). The expression of ZF-ED was represented as the FLAG-tag expression relative to *GAPDH* (A), and normalized to ZF-NOED (B and C). Dot plots represent the mean and variation of three independent experiments. Statistical significance was analyzed using one-way ANOVA

followed by Bonferroni's Multiple Comparison Test (#P<0.05, ##P<0.01, ###P<0.001, compared between two indicated columns).

Figure 8 Quantification of the changes of SPDEF protein levels in A549 cells treated with *SPDEF* targeted DNMT3A and G9a. A549 cells were treated with ZF fused with different effector domains (SKD, DNMT3A, G9a, and respective mutant DNMT3A E74A and G9a W1050A). (A) Protein expression of SPDEF was assessed by Western blot. An anti-GAPDH antibody was used as a loading control. Blot pictures shown are representative of three independent experiments. (B) Densitometric values of SPDEF were normalized against the loading control, GAPDH. The relative level (ratio to mock) of SPDEF was shown with the average of three independent experiments. Statistical significance was analyzed using one-way ANOVA followed by Bonferroni's Multiple Comparison Test (*P<0.05, **P<0.01, compared to empty vector).

Figure 9 Quantification of MUC5AC positive A549 cells after treatment with *SPDEF* targeted DNMT3A and G9a. A549 cells were treated with ZFs fused with different effector domains (SKD, DNMT3A, G9a, and respective mutant DNMT3A E74A and G9a W1050A) and grown on coverslips. Immunochemistry staining for MUC5AC was quantified to negative, weak-positive and strong-positive in a blinded fashion. (A) Percentage of MUC5AC positive cells in the total cell populations. (B) Percentage of MUC5AC strong-positive cells in the total cell populations. Results are represented as mean and variation of three independent experiments. Statistical significance was analyzed using one-way ANOVA followed by Bonferroni's Multiple Comparison Test (*P<0.05, compared to empty vector).

Figure 10 Expression of irrelevant genes after A549 cells treated with ZF fused to different effector domain (DNMT3A, G9a, and respective mutant DNMT3A E74A and G9a W1050A).

The expression of *PLOD2* (A), *TP53* (B), *RELA* (C) and *CDKN1A* (D) was relative to *ACTB*. The dot plots represent the mean and variation of three independent experiments.

Figure 11 Sustained gene repression by means of epigenetic editing using the CRISPR-dCas9 system. (A) Schematic representation of the experimental setup with the stable MCF7 cells. mRNA level of *SPDEF* determined by quantitative RT-PCR on MCF7 stable cells with dCas9-(B) SKD, (C) G9a and its mutant and Suv39h1 (D) SET and its mutant and (E) DNMT3a3L and its mutant. Results are represented as average (±SEM) of three independent experiments.

References

1. **Amabile A, Migliara A, Capasso P, Biffi M, Cittaro D, Naldini L, and Lombardo A**. Inheritable Silencing of Endogenous Genes by Hit-and-Run Targeted Epigenetic Editing. *Cell* 167: 219-232 e214, 2016.
2. **Bintu L, Yong J, Antebi YE, McCue K, Kazuki Y, Uno N, Oshimura M, and Elowitz MB**. Dynamics of epigenetic regulation at the single-cell level. *Science* 351: 720-724, 2016.
3. **Brenet F, Moh M, Funk P, Feierstein E, Viale AJ, Socci ND, and Scandura JM**. DNA methylation of the first exon is tightly linked to transcriptional silencing. *PloS one* 6: e14524, 2011.
4. **Cano-Rodriguez D, Gjaltema RA, Jilderda LJ, Jellema P, Dokter-Fokkens J, Ruiters MH, and Rots MG**. Writing of H3K4Me3 overcomes epigenetic silencing in a sustained but context-dependent manner. *Nature communications* 7: 12284, 2016.
5. **Cano-Rodriguez D, and Rots MG**. Epigenetic Editing: On the Verge of Reprogramming Gene Expression at Will. *Current Genetic Medicine Reports* 1-10, 2016.
6. **Chen G, Korfhagen TR, Xu Y, Kitzmiller J, Wert SE, Maeda Y, Gregorieff A, Clevers H, and Whitsett JA**. SPDEF is required for mouse pulmonary goblet cell differentiation and regulates a network of genes associated with mucus production. *Journal of Clinical Investigation* 119: 2914-2924, 2009.
7. **Chen H, Kazemier HG, de Groote ML, Ruiters MH, Xu GL, and Rots MG**. Induced DNA demethylation by targeting Ten-Eleven Translocation 2 to the human ICAM-1 promoter. *Nucleic acids research* 42: 1563-1574, 2014.
8. **de Groote ML, Verschure PJ, and Rots MG**. Epigenetic Editing: targeted rewriting of epigenetic marks to modulate expression of selected target genes. *Nucleic acids research* 40: 10596-10613, 2012.
9. **Fahy JV, and Dickey BF**. Airway mucus function and dysfunction. *The New England journal of medicine* 363: 2233-2247, 2010.
10. **Falahi F, Huisman C, Kazemier HG, van der Vlies P, Kok K, Hospers GA, and Rots MG**. Towards sustained silencing of HER2/neu in cancer by epigenetic editing. *Molecular cancer research : MCR* 11: 1029-1039, 2013.
11. **Gao W, Li L, Wang Y, Zhang S, Adcock IM, Barnes PJ, Huang M, and Yao X**. Bronchial epithelial cells: The key effector cells in the pathogenesis of chronic obstructive pulmonary disease? *Respirology* 20: 722-729, 2015.
12. **Gjaltema RAF, de Rond S, Rots MG, and Bank RA**. Procollagen Lysyl Hydroxylase 2 Expression Is Regulated by an Alternative Downstream Transforming Growth Factor beta-1 Activation Mechanism. *Journal of Biological Chemistry* 290: 28465-28476, 2015.
13. **Gowher H, Loutchanwoot P, Vorobjeva O, Handa V, Jurkowska RZ, Jurkowski TP, and Jeltsch A**. Mutational analysis of the catalytic domain of the murine Dnmt3a DNA-(cytosine C5)-methyltransferase. *Journal of molecular biology* 357: 928-941, 2006.
14. **Hathaway NA, Bell O, Hodges C, Miller EL, Neel DS, and Crabtree GR**. Dynamics and memory of heterochromatin in living cells. *Cell* 149: 1447-1460, 2012.
15. **Heijink IH, Brandenburg SM, Noordhoek JA, Postma DS, Slebos D-J, and van Oosterhout AJM**. Characterisation of cell adhesion in airway epithelial cell types using electric cell–substrate impedance sensing. *European Respiratory Journal* 35: 894-903, 2010.
16. **Huisman C, Wisman GB, Kazemier HG, van Vugt MA, van der Zee AG, Schuuring E, and Rots MG**. Functional validation of putative tumor suppressor gene

599 C13ORF18 in cervical cancer by Artificial Transcription Factors. *Molecular oncology* 7: 669-
600 679, 2013.
601 17. **Jurkowski TP, Ravichandran M, and Stepper P**. Synthetic epigenetics—towards
602 intelligent control of epigenetic states and cell identity. *Clinical epigenetics* 7: 18, 2015.
603 18. **Kearns NA, Genga RM, Enuameh MS, Garber M, Wolfe SA, and Maehr R**. Cas9
604 effector-mediated regulation of transcription and differentiation in human pluripotent stem
605 cells. *Development* 141: 219-223, 2014.
606 19. **Kungulovski G, Nunna S, Thomas M, Zanger UM, Reinhardt R, and Jeltsch A**.
607 Targeted epigenome editing of an endogenous locus with chromatin modifiers is not stably
608 maintained. *Epigenetics & chromatin* 8: 12, 2015.
609 20. **Larson MH, Gilbert LA, Wang X, Lim WA, Weissman JS, and Qi LS**. CRISPR
610 interference (CRISPRi) for sequence-specific control of gene expression. *Nat Protoc* 8: 2180-
611 2196, 2013.
612 21. **Martin C, Frija-Masson J, and Burgel PR**. Targeting mucus hypersecretion: new
613 therapeutic opportunities for COPD? *Drugs* 74: 1073-1089, 2014.
614 22. **McCauley HA, and Guasch G**. Three cheers for the goblet cell: maintaining
615 homeostasis in mucosal epithelia. *Trends in molecular medicine* 21: 492-503, 2015.
616 23. **Miravitlles M**. Cough and sputum production as risk factors for poor outcomes in
617 patients with COPD. *Resp Med* 105: 1118-1128, 2011.
618 24. **Nunna S, Reinhardt R, Ragozin S, and Jeltsch A**. Targeted methylation of the
619 epithelial cell adhesion molecule (EpCAM) promoter to silence its expression in ovarian
620 cancer cells. *PloS one* 9: e87703, 2014.
621 25. **Park KS, Korfhagen TR, Bruno MD, Kitzmiller JA, Wan H, Wert SE, Khurana**
622 **Hershey GK, Chen G, and Whitsett JA**. SPDEF regulates goblet cell hyperplasia in the
623 airway epithelium. *J Clin Invest* 117: 978-988, 2007.
624 26. **Rajavelu P, Chen G, Xu Y, Kitzmiller JA, Korfhagen TR, and Whitsett JA**.
625 Airway epithelial SPDEF integrates goblet cell differentiation and pulmonary Th2
626 inflammation. *J Clin Invest* 125: 2021-2031, 2015.
627 27. **Ramos FL, Krahnke JS, and Kim V**. Clinical issues of mucus accumulation in
628 COPD. *International journal of chronic obstructive pulmonary disease* 9: 139-150, 2014.
629 28. **Rivenbark AG, Stolzenburg S, Beltran AS, Yuan X, Rots MG, Strahl BD, and**
630 **Blancafort P**. Epigenetic reprogramming of cancer cells via targeted DNA methylation.
631 *Epigenetics* 7: 350-360, 2012.
632 29. **Siddique AN, Nunna S, Rajavelu A, Zhang Y, Jurkowska RZ, Reinhardt R, Rots**
633 **MG, Ragozin S, Jurkowski TP, and Jeltsch A**. Targeted methylation and gene silencing of
634 VEGF-A in human cells by using a designed Dnmt3a-Dnmt3L single-chain fusion protein
635 with increased DNA methylation activity. *Journal of molecular biology* 425: 479-491, 2013.
636 30. **Stepper P, Kungulovski G, Jurkowska RZ, Chandra T, Krueger F, Reinhardt R,**
637 **Reik W, Jeltsch A, and Jurkowski TP**. Efficient targeted DNA methylation with chimeric
638 dCas9-Dnmt3a-Dnmt3L methyltransferase. *Nucleic acids research* 2016.
639 31. **Stolzenburg S, Beltran AS, Swift-Scanlan T, Rivenbark AG, Rashwan R, and**
640 **Blancafort P**. Stable oncogenic silencing in vivo by programmable and targeted de novo
641 DNA methylation in breast cancer. *Oncogene* 34: 5427-5435, 2015.
642 32. **Stolzenburg S, Rots MG, Beltran AS, Rivenbark AG, Yuan X, Qian H, Strahl**
643 **BD, and Blancafort P**. Targeted silencing of the oncogenic transcription factor SOX2 in
644 breast cancer. *Nucleic acids research* 40: 6725-6740, 2012.
645 33. **Thakore PI, Black JB, Hilton IB, and Gersbach CA**. Editing the epigenome:
646 technologies for programmable transcription and epigenetic modulation. *Nature methods* 13:
647 127-137, 2016.

34. **Thomson NC, Chaudhuri R, Messow CM, Spears M, MacNee W, Connell M, Murchison JT, Sproule M, and McSharry C**. Chronic cough and sputum production are associated with worse clinical outcomes in stable asthma. *Respir Med* 107: 1501-1508, 2013.
35. **Wang G, Xu Z, Wang R, Al-Hijji M, Salit J, Strulovici-Barel Y, Tilley AE, Mezey JG, and Crystal RG**. Genes associated with MUC5AC expression in small airway epithelium of human smokers and non-smokers. *BMC medical genomics* 5: 21, 2012.
36. **Yu H, Li Q, Kolosov VP, Perelman JM, and Zhou X**. Interleukin-13 induces mucin 5AC production involving STAT6/SPDEF in human airway epithelial cells. *Cell communication & adhesion* 17: 83-92, 2010.

Figure 1

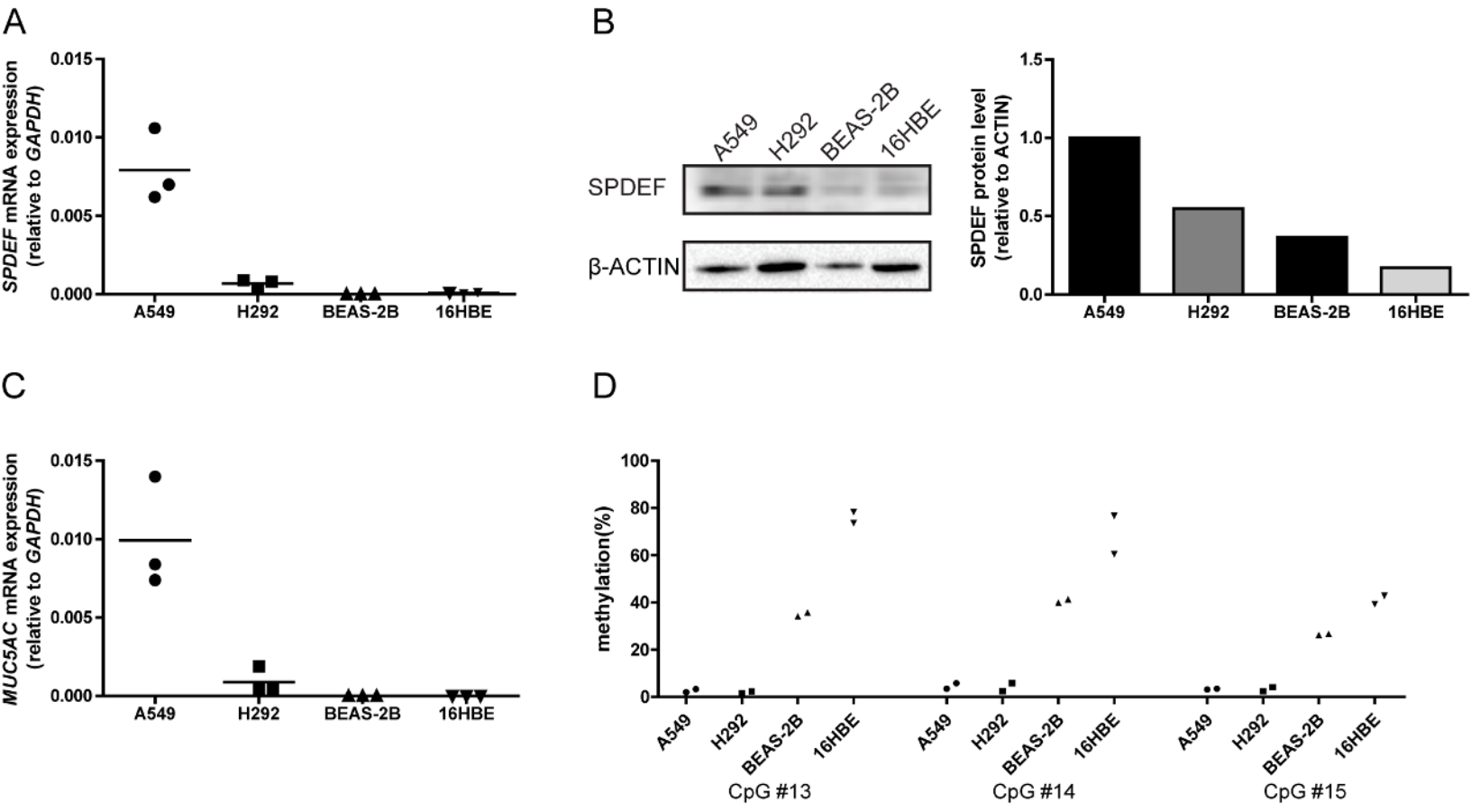
A
SPDEF mRNA expression (relative to GAPDH)
0.015
0.010
0.005
0.000
A549
H292
BEAS-2B
16HBE
B
A549
H292
BEAS-2B
16HBE
SPDEF
β-ACTIN
SPDEF protein level (relative to ACTIN)
1.5
1.0
0.5
0.0
A549
H292
BEAS-2B
16HBE
C
MUC5AC mRNA expression (relative to GAPDH)
0.015
0.010
0.005
0.000
A549
H292
BEAS-2B
16HBE
D
methylation(%)
100
80
60
40
20
0
A549
H292
BEAS-2B
16HBE
CpG #13
CpG #14
CpG #15

Figure 2

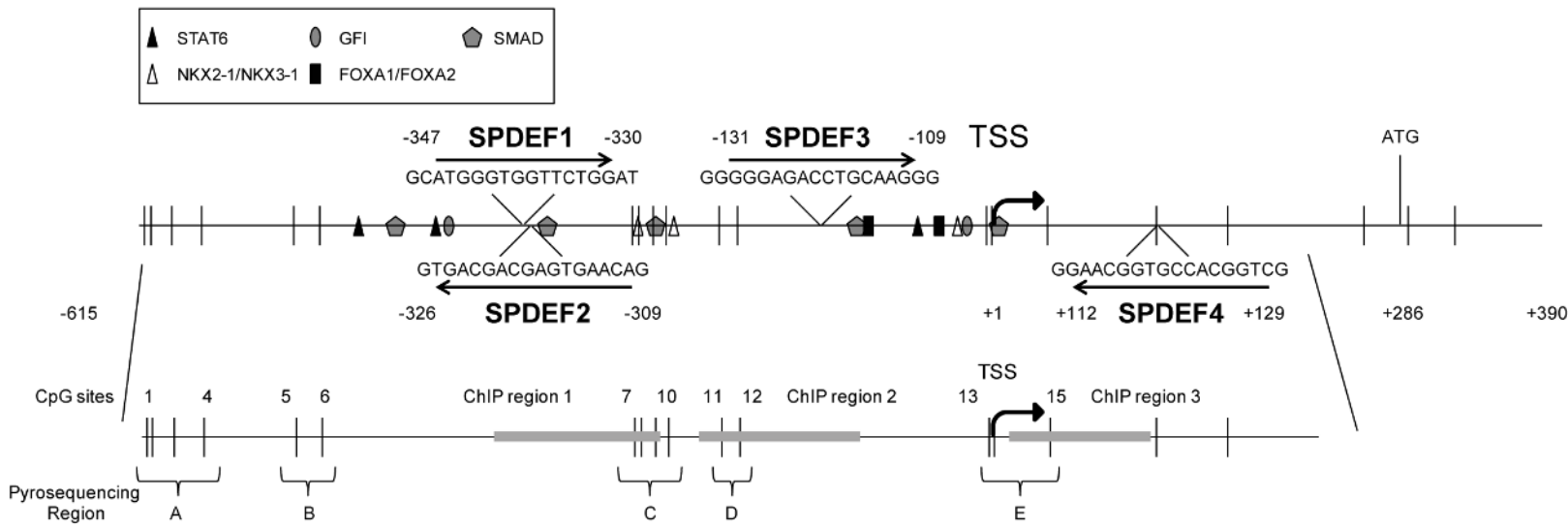
A
STAT6
GFI
SMAD
NKX2-1/NKX3-1
FOXA1/FOXA2
-347
SPDEF1
-330
GCATGGGTGGTTCTGGAT
-131
SPDEF3
-109
GGGGGAGACCTGCAAGGG
TSS
ATG
GTGACGACGAGTGAACAG
GGAACGGTGCCACGGTCG
-615
-326
SPDEF2
-309
+1
+112
SPDEF4
+129
+286
+390
CpG sites
1
4
5
6
ChIP region 1
7
10
11
12
ChIP region 2
13
TSS
15
ChIP region 3
Pyrosequencing Region
A
B
C
D
E

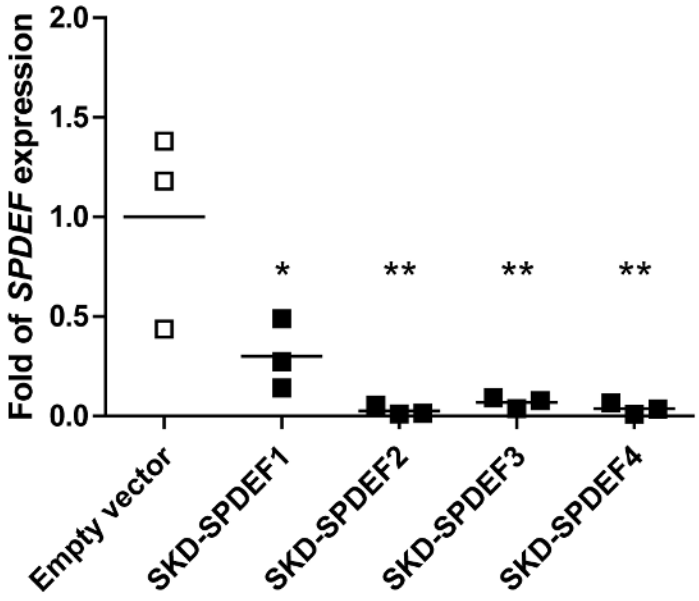
B
Fold of SPDEF expression
2.0
1.5
1.0
0.5
0.0
*
**
**
**
Empty vector
SKD-SPDEF1
SKD-SPDEF2
SKD-SPDEF3
SKD-SPDEF4

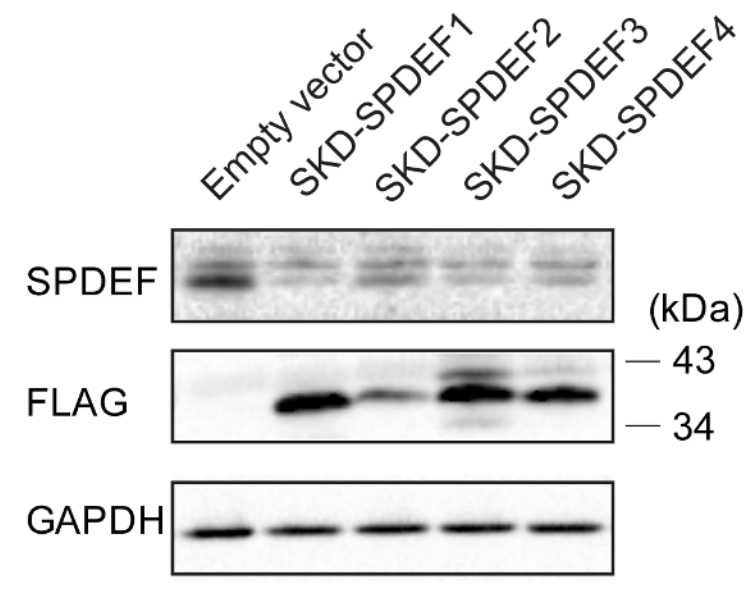
C
Empty vector
SKD-SPDEF1
SKD-SPDEF2
SKD-SPDEF3
SKD-SPDEF4
SPDEF
FLAG
GAPDH
(kDa)
43
34

Figure 3

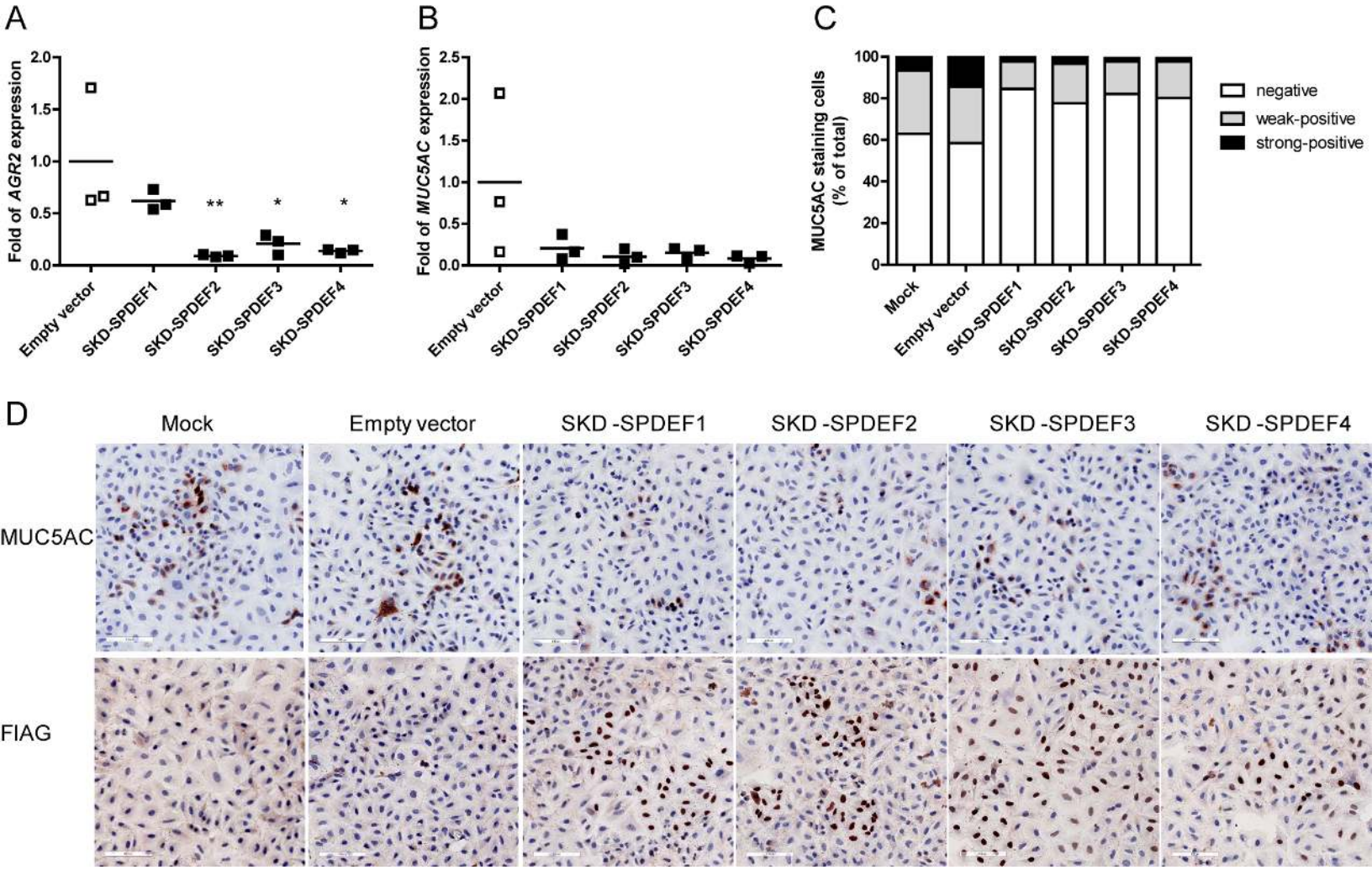
A
Fold of AGR2 expression
2.0
1.5
1.0
0.5
0.0
**
*
*
Empty vector
SKD-SPDEF1
SKD-SPDEF2
SKD-SPDEF3
SKD-SPDEF4
B
Fold of MUC5AC expression
2.5
2.0
1.5
1.0
0.5
0.0
Empty vector
SKD-SPDEF1
SKD-SPDEF2
SKD-SPDEF3
SKD-SPDEF4
C
MUC5AC staining cells (% of total)
100
80
60
40
20
0
Mock
Empty vector
SKD-SPDEF1
SKD-SPDEF2
SKD-SPDEF3
SKD-SPDEF4
negative
weak-positive
strong-positive

D
Mock
Empty vector
SKD -SPDEF1
SKD -SPDEF2
SKD -SPDEF3
SKD -SPDEF4
MUC5AC
FIAG

Figure 4

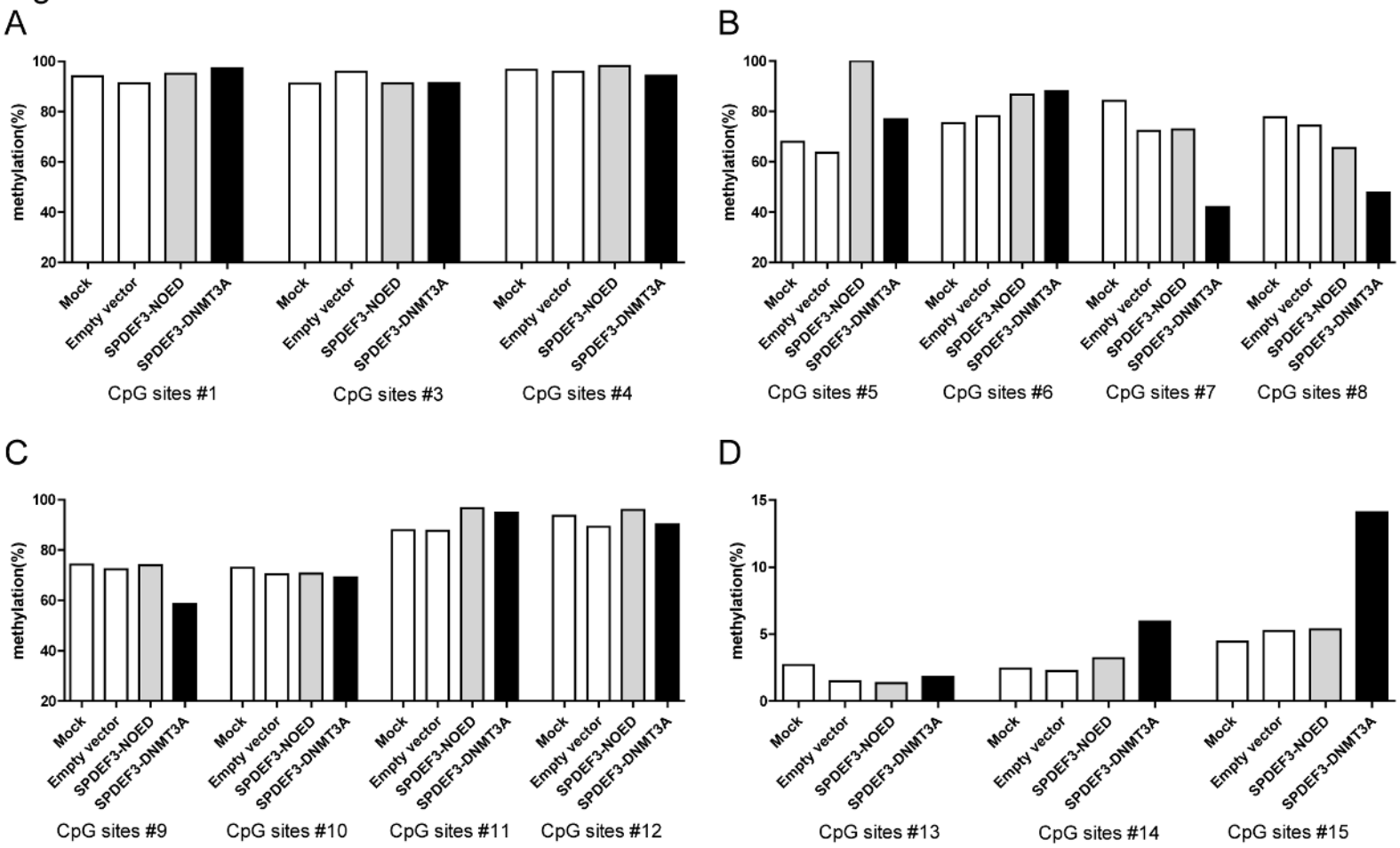
A
B
C
D
methylation(%)
Mock
Empty vector
SPDEF3-NOED
SPDEF3-DNMT3A
CpG sites #1
CpG sites #3
CpG sites #4
CpG sites #5
CpG sites #6
CpG sites #7
CpG sites #8
CpG sites #9
CpG sites #10
CpG sites #11
CpG sites #12
CpG sites #13
CpG sites #14
CpG sites #15

Figure 5

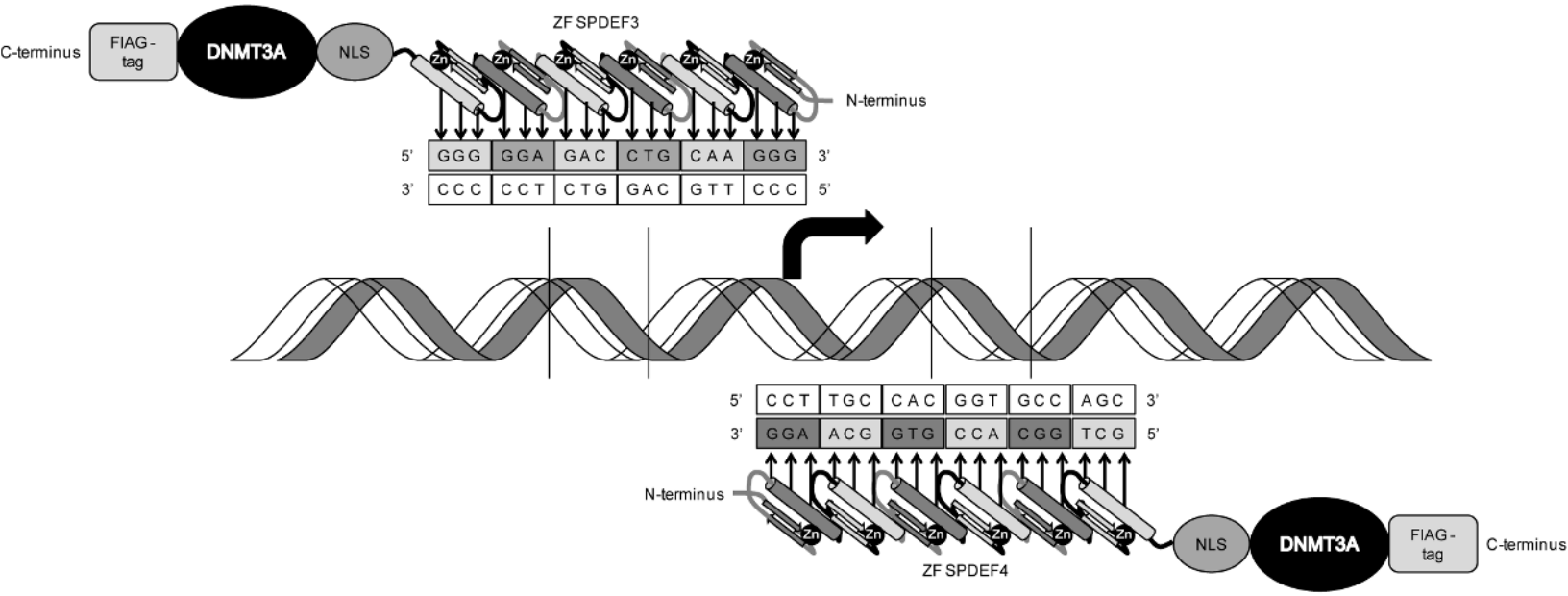
A
C-terminus
FIAG-tag
DNMT3A
NLS
ZF SPDEF3
N-terminus
5' GGG GGA GAC CTG CAA GGG 3'
3' CCC CCT CTG GAC GTT CCC 5'
5' CCT TGC CAC GGT GCC AGC 3'
3' GGA ACG GTG CCA CGG TCG 5'
N-terminus
ZF SPDEF4
NLS
DNMT3A
FIAG-tag
C-terminus

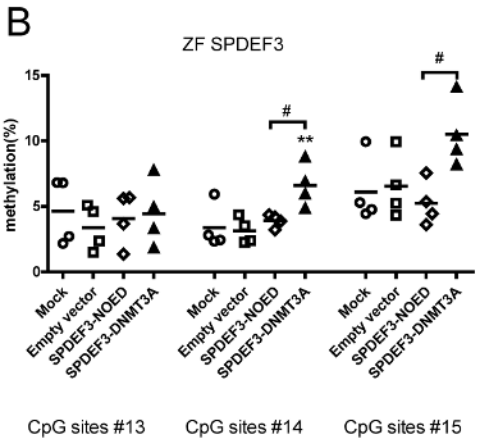
B
ZF SPDEF3
methylation(%)
Mock
Empty vector
SPDEF3-NOED
SPDEF3-DNMT3A
CpG sites #13
CpG sites #14
CpG sites #15

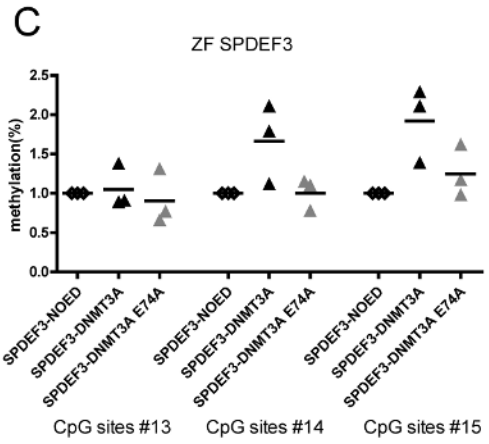
C
ZF SPDEF3
methylation(%)
SPDEF3-NOED
SPDEF3-DNMT3A
SPDEF3-DNMT3A E74A
CpG sites #13
CpG sites #14
CpG sites #15

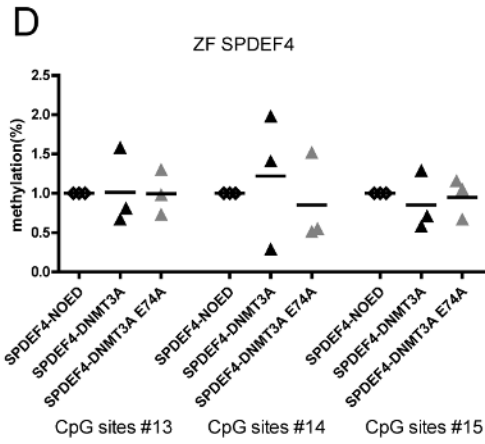
D
ZF SPDEF4
methylation(%)
SPDEF4-NOED
SPDEF4-DNMT3A
SPDEF4-DNMT3A E74A
CpG sites #13
CpG sites #14
CpG sites #15

Figure 6

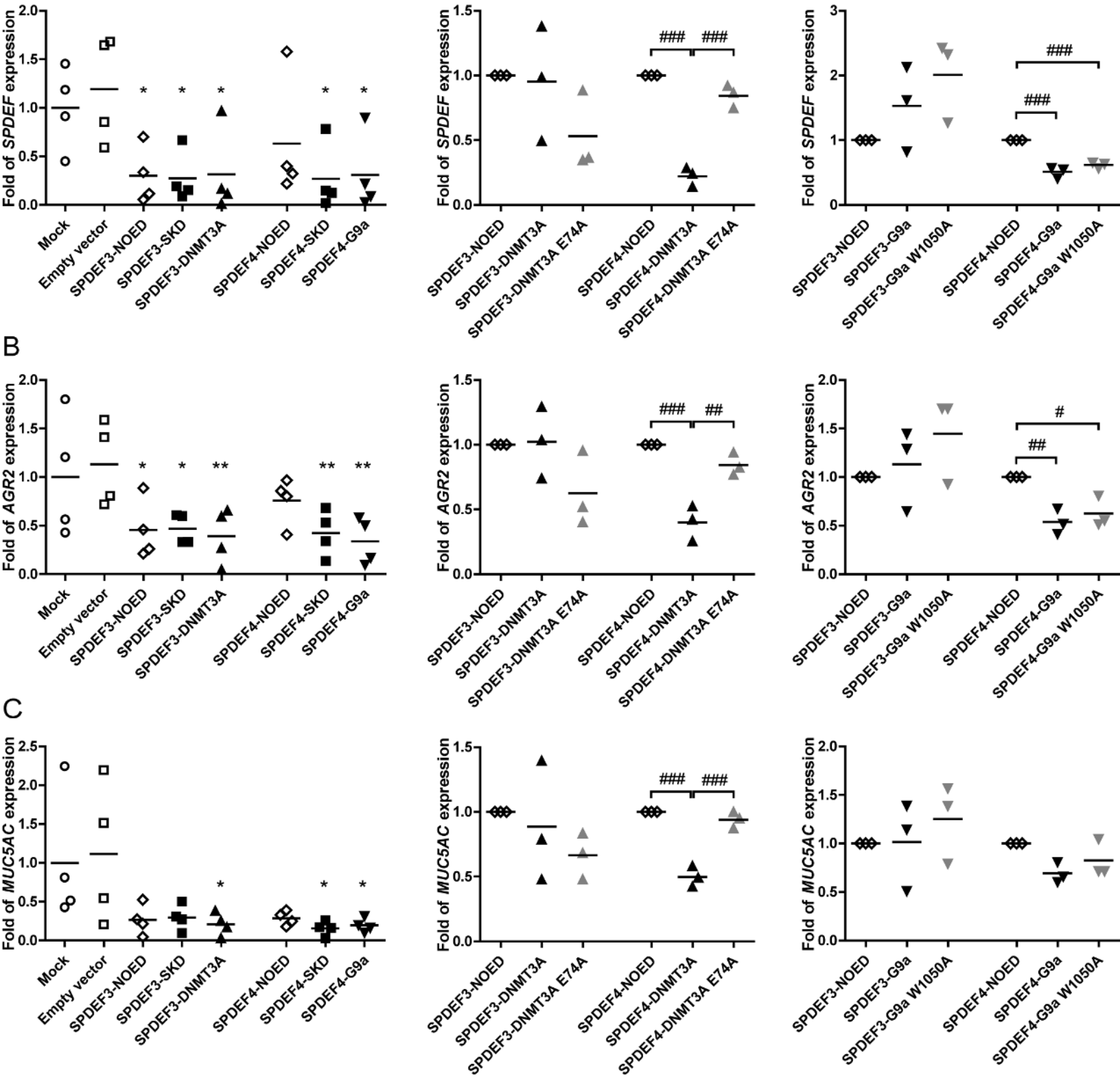
A
Fold of SPDEF expression
Mock
Empty vector
SPDEF3-NOED
SPDEF3-SKD
SPDEF3-DNMT3A
SPDEF4-NOED
SPDEF4-SKD
SPDEF4-G9a
SPDEF3-DNMT3A E74A
SPDEF4-DNMT3A
SPDEF4-DNMT3A E74A
SPDEF3-G9a
SPDEF3-G9a W1050A
SPDEF4-G9a
SPDEF4-G9a W1050A
B
Fold of AGR2 expression
C
Fold of MUC5AC expression

Figure 7

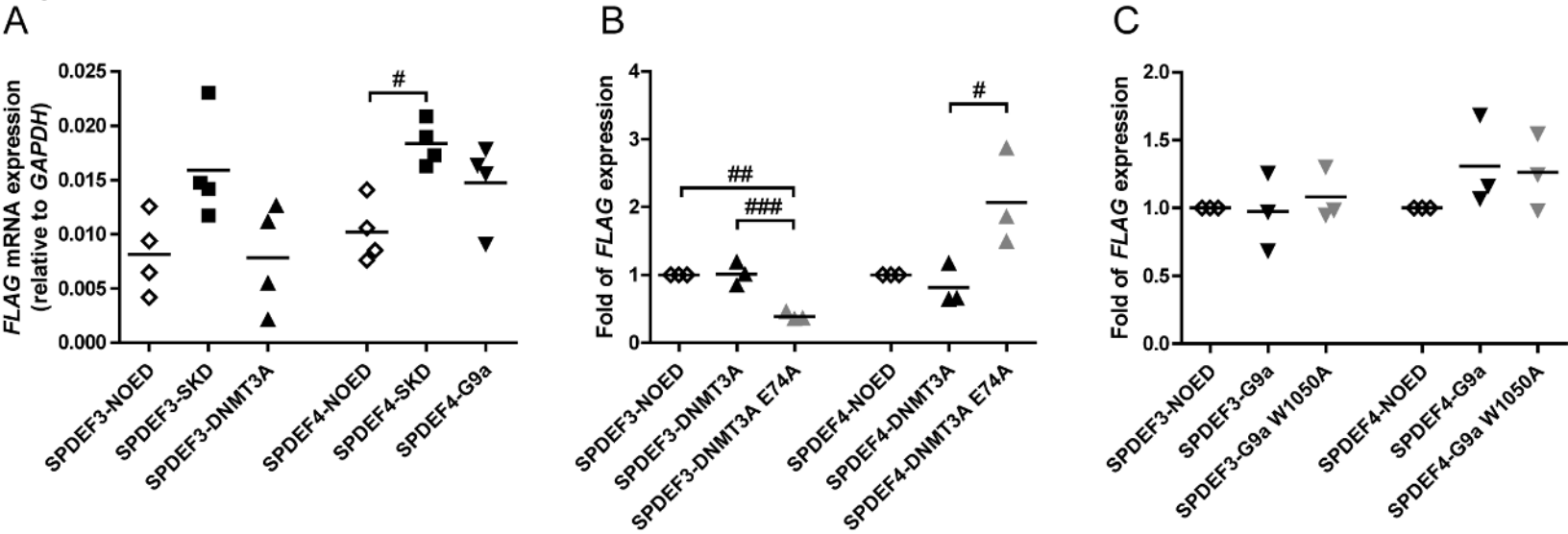
A
FLAG mRNA expression (relative to GAPDH)
0.025
0.020
0.015
0.010
0.005
0.000
#
SPDEF3-NOED
SPDEF3-SKD
SPDEF3-DNMT3A
SPDEF4-NOED
SPDEF4-SKD
SPDEF4-G9a
B
Fold of FLAG expression
4
3
2
1
0
##
###
#
SPDEF3-NOED
SPDEF3-DNMT3A
SPDEF3-DNMT3A E74A
SPDEF4-NOED
SPDEF4-DNMT3A
SPDEF4-DNMT3A E74A
C
Fold of FLAG expression
2.0
1.5
1.0
0.5
0.0
SPDEF3-NOED
SPDEF3-G9a
SPDEF3-G9a W1050A
SPDEF4-NOED
SPDEF4-G9a
SPDEF4-G9a W1050A

Figure 8

A

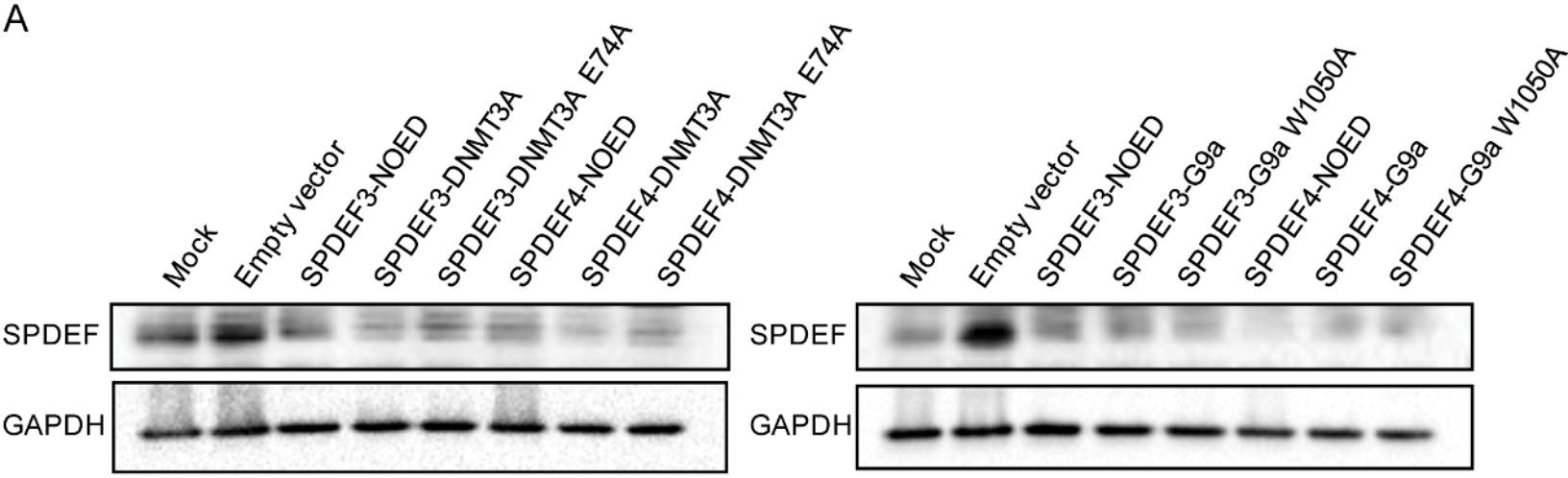
Mock
Empty vector
SPDEF3-NOED
SPDEF3-DNMT3A
SPDEF3-DNMT3A E74A
SPDEF4-NOED
SPDEF4-DNMT3A
SPDEF4-DNMT3A E74A
SPDEF
GAPDH
Mock
Empty vector
SPDEF3-NOED
SPDEF3-G9a
SPDEF3-G9a W1050A
SPDEF4-NOED
SPDEF4-G9a
SPDEF4-G9a W1050A
SPDEF
GAPDH

B

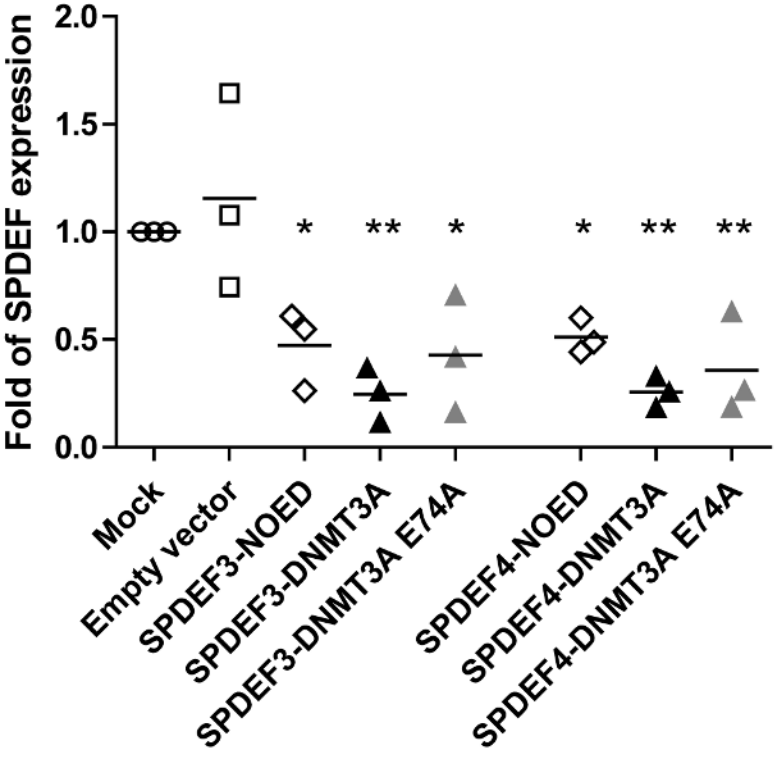
Fold of SPDEF expression
2.0
1.5
1.0
0.5
0.0
*
**
*
*
**
**
Mock
Empty vector
SPDEF3-NOED
SPDEF3-DNMT3A
SPDEF3-DNMT3A E74A
SPDEF4-NOED
SPDEF4-DNMT3A
SPDEF4-DNMT3A E74A

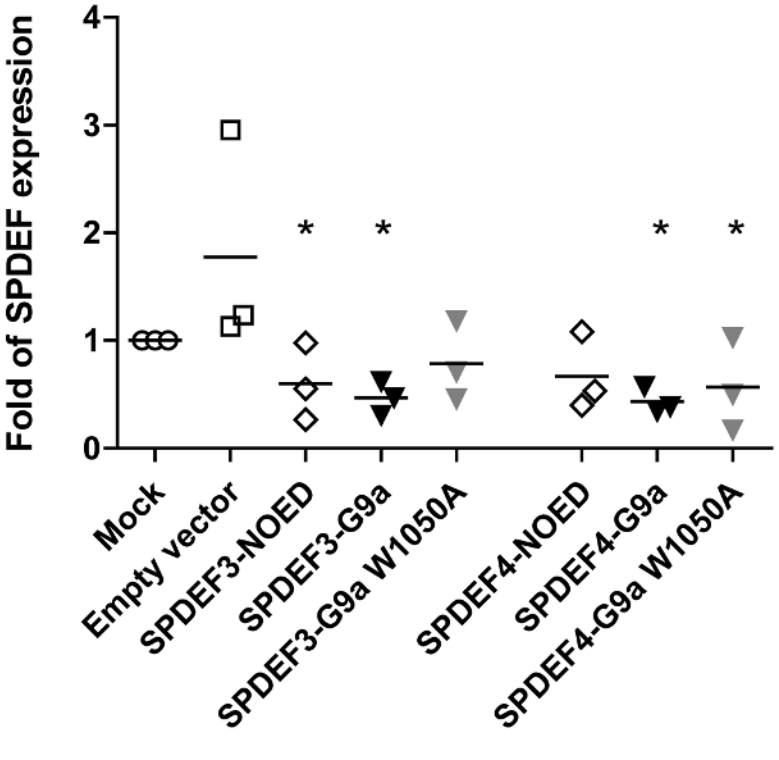
Fold of SPDEF expression
4
3
2
1
0
*
*
*
*
Mock
Empty vector
SPDEF3-NOED
SPDEF3-G9a
SPDEF3-G9a W1050A
SPDEF4-NOED
SPDEF4-G9a
SPDEF4-G9a W1050A

Figure 9

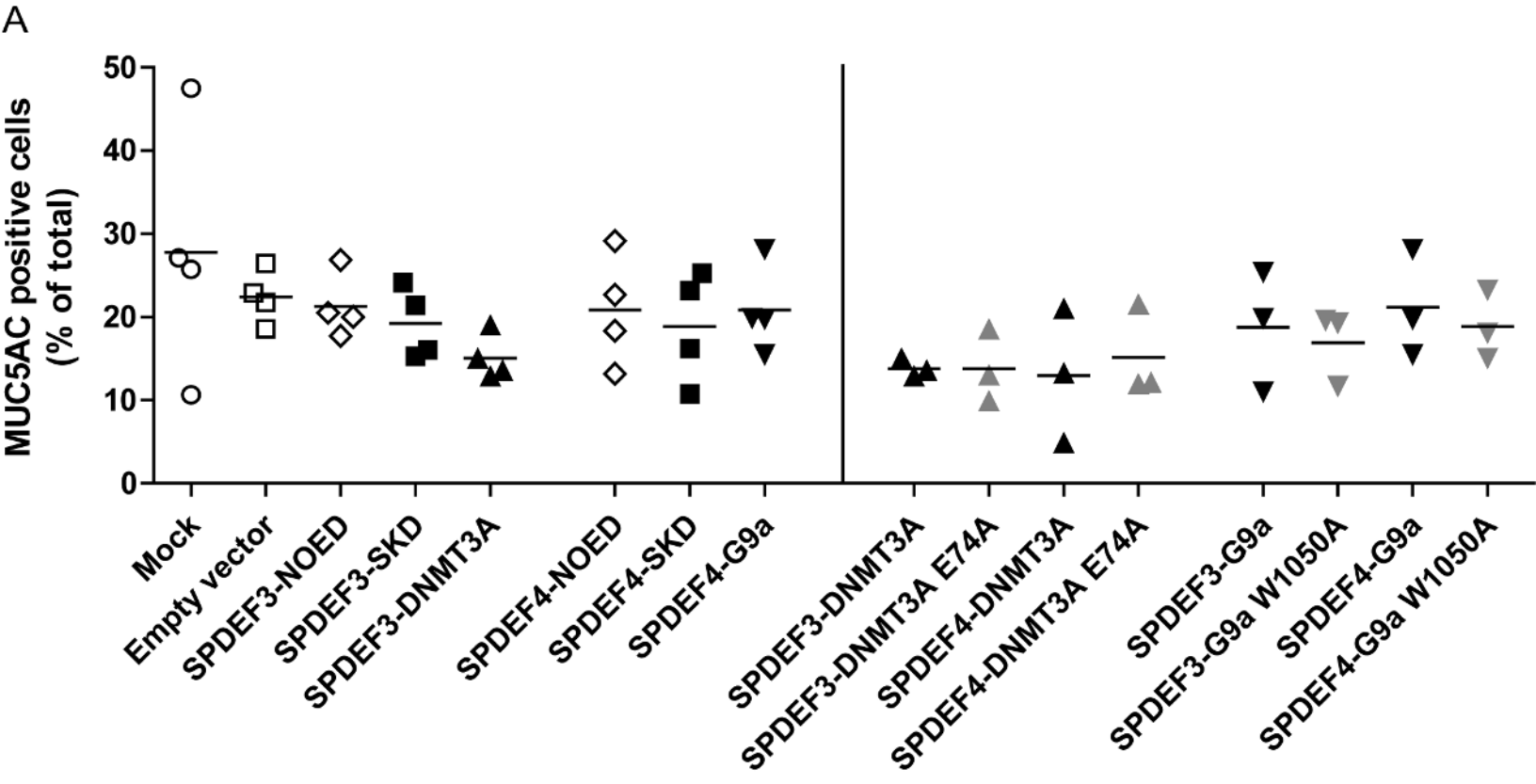
A
MUC5AC positive cells
(% of total)
50
40
30
20
10
0
Mock
Empty vector
SPDEF3-NOED
SPDEF3-SKD
SPDEF3-DNMT3A
SPDEF4-NOED
SPDEF4-SKD
SPDEF4-G9a
SPDEF3-DNMT3A
SPDEF3-DNMT3A E74A
SPDEF4-DNMT3A
SPDEF4-DNMT3A E74A
SPDEF3-G9a
SPDEF3-G9a W1050A
SPDEF4-G9a
SPDEF4-G9a W1050A

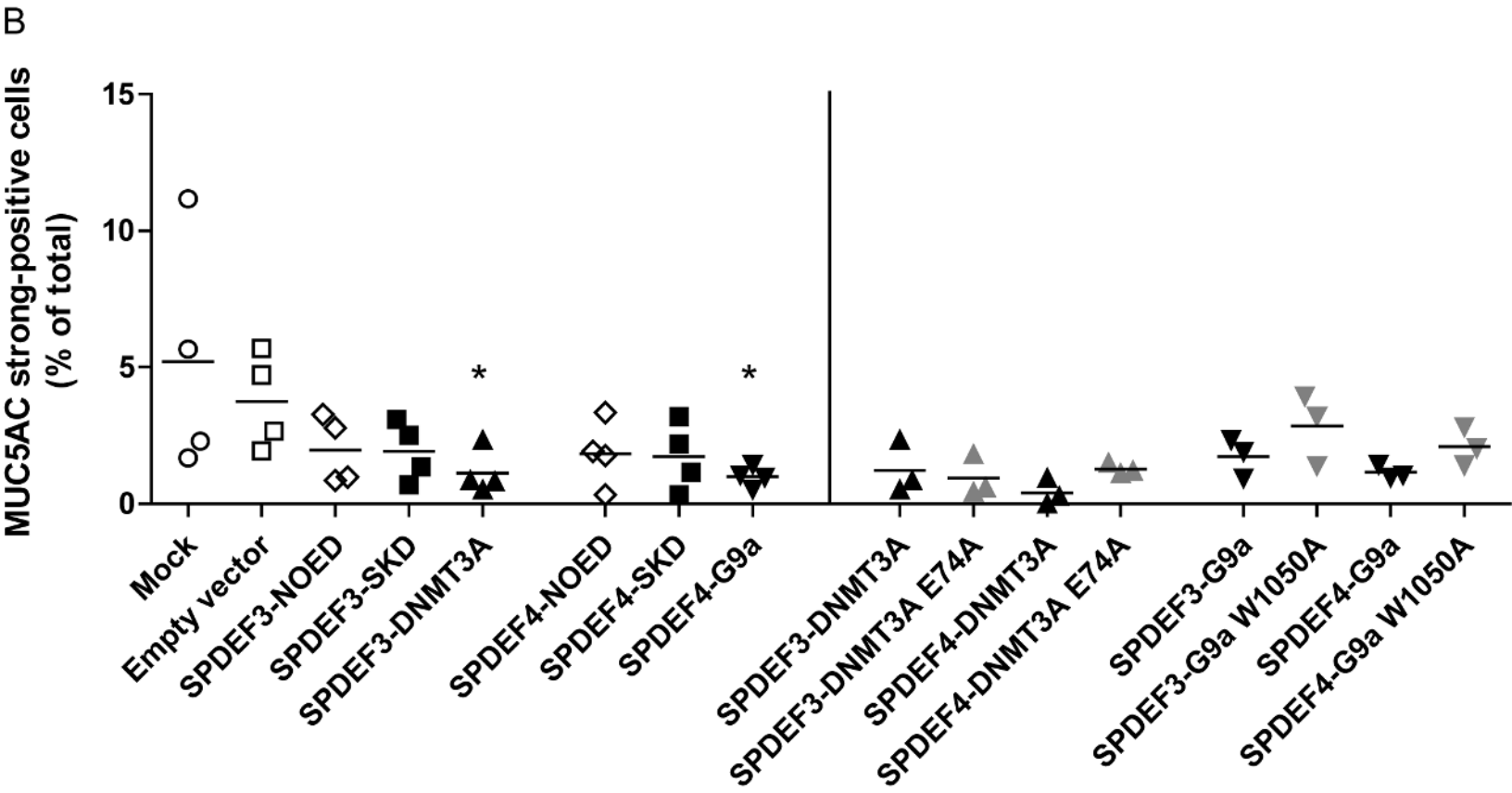
B
MUC5AC strong-positive cells
(% of total)
15
10
5
0
*
*
Mock
Empty vector
SPDEF3-NOED
SPDEF3-SKD
SPDEF3-DNMT3A
SPDEF4-NOED
SPDEF4-SKD
SPDEF4-G9a
SPDEF3-DNMT3A
SPDEF3-DNMT3A E74A
SPDEF4-DNMT3A
SPDEF4-DNMT3A E74A
SPDEF3-G9a
SPDEF3-G9a W1050A
SPDEF4-G9a
SPDEF4-G9a W1050A

Figure 10

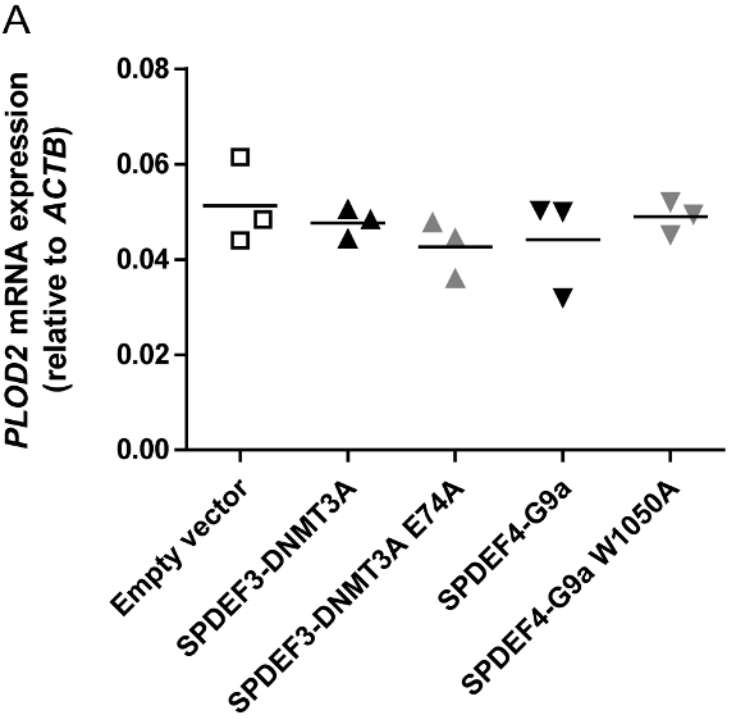
A
PLOD2 mRNA expression (relative to ACTB)
0.08
0.06
0.04
0.02
0.00
Empty vector
SPDEF3-DNMT3A
SPDEF3-DNMT3A E74A
SPDEF4-G9a
SPDEF4-G9a W1050A

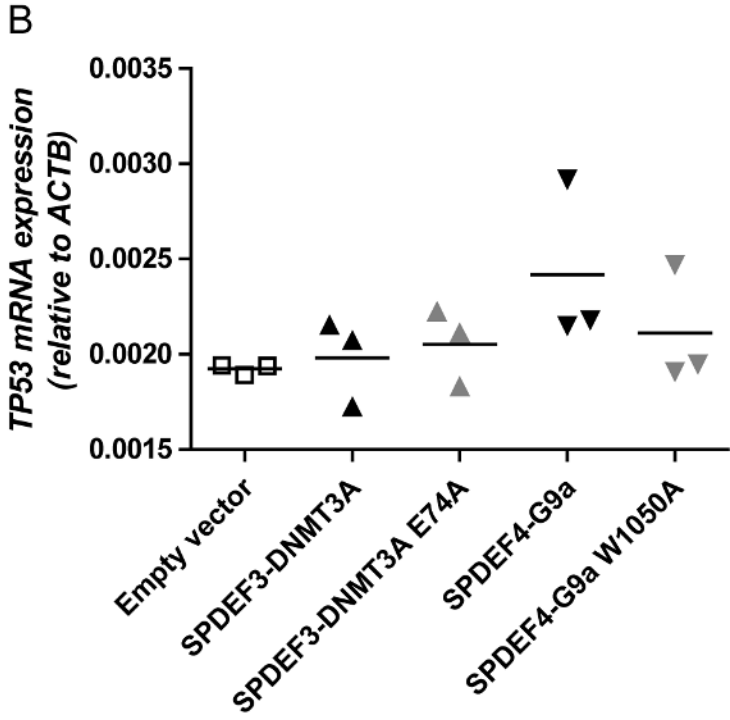
B
TP53 mRNA expression (relative to ACTB)
0.0035
0.0030
0.0025
0.0020
0.0015
Empty vector
SPDEF3-DNMT3A
SPDEF3-DNMT3A E74A
SPDEF4-G9a
SPDEF4-G9a W1050A

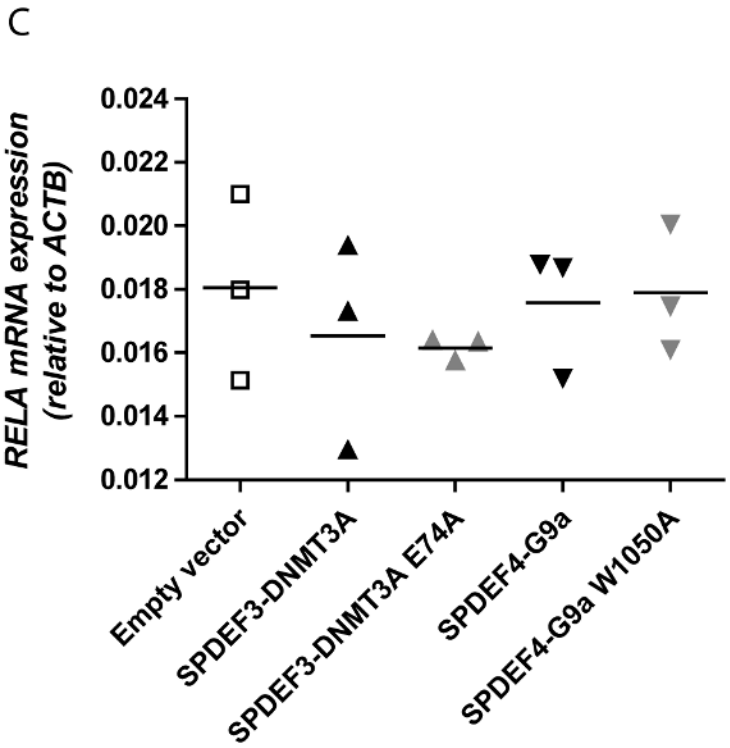
C
RELA mRNA expression (relative to ACTB)
0.024
0.022
0.020
0.018
0.016
0.014
0.012
Empty vector
SPDEF3-DNMT3A
SPDEF3-DNMT3A E74A
SPDEF4-G9a
SPDEF4-G9a W1050A

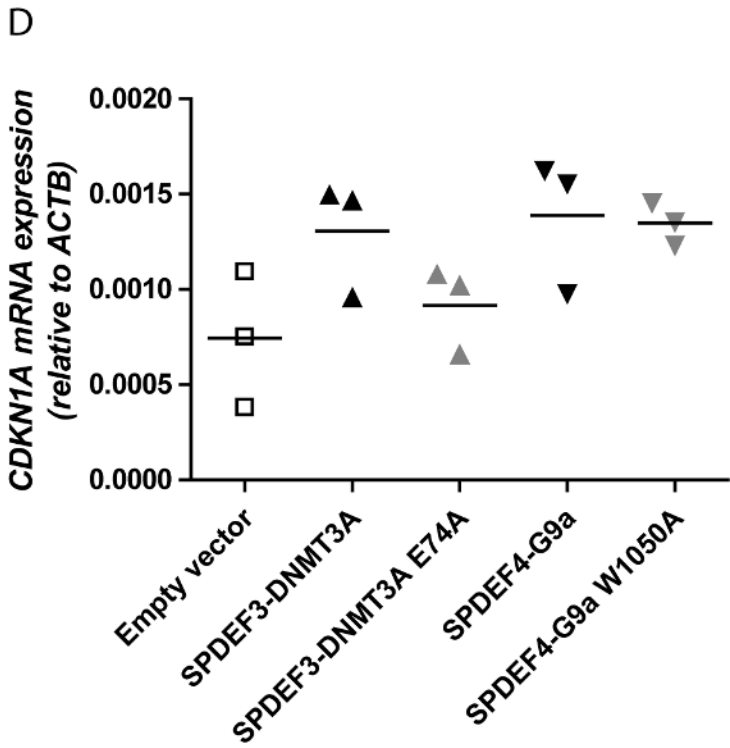
D
CDKN1A mRNA expression (relative to ACTB)
0.0020
0.0015
0.0010
0.0005
0.0000
Empty vector
SPDEF3-DNMT3A
SPDEF3-DNMT3A E74A
SPDEF4-G9a
SPDEF4-G9a W1050A

Figure 11

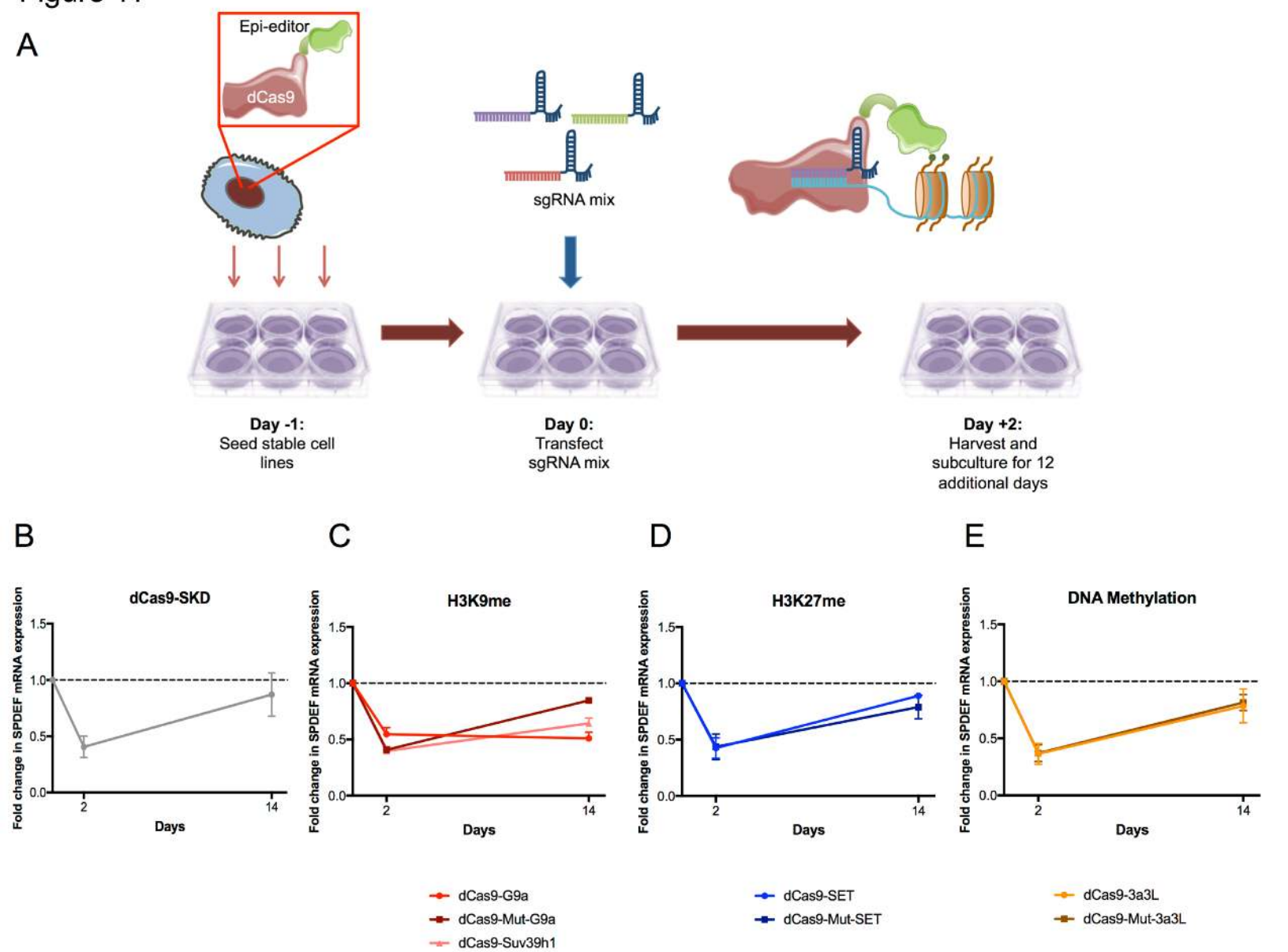
A
Epi-editor
dCas9
sgRNA mix
Day -1:
Seed stable cell lines
Day 0:
Transfect sgRNA mix
Day +2:
Harvest and subculture for 12 additional days
B
dCas9-SKD
C
H3K9me
D
H3K27me
E
DNA Methylation
Fold change in SPDEF mRNA expression
1.5
1.0
0.5
0.0
2
14
Days
dCas9-G9a
dCas9-Mut-G9a
dCas9-Suv39h1
dCas9-SET
dCas9-Mut-SET
dCas9-3a3L
dCas9-Mut-3a3L